npj | biofilms and microbiomes

Article

Published in partnership with Nanyang Technological University

https://doi.org/10.1038/s41522-025-00672-3

Gut commensals-derived succinate impels colonic inflammation in ulcerative colitis

Rajdeep Dalal[1,2,3], Srikanth Sadhu[1,2], Aashima Batra[4], Sandeep Goswami[1,2], Jyotsna Dandotiya[1,2], Vinayakadas K. V[1,2], Rahul Yadav[1,2], Virendra Singh[1,2], Kartikey Chaturvedi[5], Rahul Kannan[5], Shakti Kumar[6], Yashwant Kumar[5], Deepak Kumar Rathore[1,2], Deepak B. Salunke[4,7], Vineet Ahuja[8] & Amit Awasthi[1,2] ✉

Gut microbiota-derived metabolites play a crucial role in modulating the inflammatory response in inflammatory bowel disease (IBD). In this study, we identify gut microbiota-derived succinate as a driver of inflammation in ulcerative colitis (UC) by activating succinate-responsive, colitogenic helper T (Th) cells that secrete interleukin (IL)-9. We demonstrate that colitis is associated with an increase in succinate-producing gut bacteria and decrease in succinate-metabolizing gut bacteria. Similarly, UC patients exhibit elevated levels of succinate-producing gut bacteria and luminal succinate. Intestinal colonization by succinate-producing gut bacteria or increased succinate availability, exacerbates colonic inflammation by activating colitogenic Th9 cells. In contrast, intestinal colonization by succinate-metabolizing gut bacteria, blocking succinate receptor signaling with an antagonist, or neutralizing IL-9 with an anti-IL-9 antibody alleviates inflammation by reducing colitogenic Th9 cells. Our findings underscore the role of gut microbiota-derived succinate in driving colitogenic Th9 cells and suggesting its potential as a therapeutic target for treating IBD.

Inflammatory bowel disease (IBD) is a chronic disorder of the gastrointestinal tract that affects millions of people globally[1]. The pathogenesis of IBD is multifaceted, driven by the interplay between genetic predisposition, environmental factors, and immune dysregulation, particularly involvement of T cells[2,3]. Dietary components have emerged as key environmental factors that modulate gut microbiota composition, thereby influencing the gut-immune axis[4]. Recent studies underscore the role of gut microbiota-derived metabolites as critical regulators of the gut-immune axis, contributing to the maintenance of intestinal homeostasis[5]. Among these, short-chain fatty acids (SCFAs) such as acetate, butyrate, propionate, and succinate are the most abundant metabolites produced by the gut microbiota[6,7]. SCFAs have gained recognition for their anti-inflammatory properties, which they exert by inhibiting histone deacetylases (HDACs) and activating G-protein-coupled receptors (GPRs), including FFA1 (GPR40), FFA2 (GPR43), FFA3 (GPR41), FFA4 (GPR120), GPR109a, and Olfr78 on intestinal epithelial cells (IECs)[8–11]. Succinate is a distinct SCFA metabolite produced by both the host and gut microbiota[7,12,13]. The primary succinate-producing gut microbiota belongs to the family *Bacteroidaceae*, while succinate-metabolizing microbes are predominantly from the family *Acidaminococcaceae*[12,14]. Cytoplasmic succinate levels increase through mitochondrial production as well as SLC-13 transporter-mediated uptake of extracellular succinate[14–16]. A recent study revealed that the uptake of colonic succinate into pro-inflammatory macrophages is regulated by Na^+-dependent succinate transporters (SLC-13) present in both macrophages and epithelial cells[14]. Additionally, the accumulation of intracellular succinate in the cytosol inhibits prolyl hydroxylase (PHD) enzymes, which

[1]Centre for Immunobiology and Immunotherapy, Translational Health Science and Technology Institute, NCR-Biotech Science Cluster, 3 rd Milestone, Faridabad-Gurgaon Expressway, Faridabad, 121001 Haryana, India. [2]Immunology Core Lab, Translational Health Science and Technology Institute, NCR Biotech Science Cluster, 3rd Milestone, Faridabad-Gurgaon Expressway, Faridabad, 121001 Haryana, India. [3]Jawaharlal Nehru University, New Delhi, India. [4]Department of Chemistry and Centre for Advanced Studies in Chemistry, Panjab University, Chandigarh, 160014, India. [5]Non-communicable disease centre, Translational Health Science and Technology Institute, NCR-Biotech Science Cluster, 3rd Milestone, Faridabad-Gurgaon Expressway, Faridabad, 121001 Haryana, India. [6]Department of Molecular Medicine & Biotechnology, Sanjay Gandhi Postgraduate Institute of Medical Sciences (SGPGIMS), Lucknow, Uttar Pradesh, India. [7]Department of Medicinal Chemistry, National Institute of Pharmaceutical Education and Research (NIPER), S.A.S. Nagar, Mohali, 160062 Punjab, India. [8]Department of Gastroenterology, All India Institute of Medical Sciences, Ansari Nagar East, New Delhi, India. ✉e-mail: aawasthi@thsti.res.in

allows the stabilization of HIF-1α-mediated Th9 cells[17,18]. Extracellular succinate, primarily produced by gut microbiota, is sensed by a G-protein-coupled receptor known as succinate receptor 1 (SUCNR1/GPR91)[19,20].

Succinate has been implicated in tissue inflammation associated with IBD, obesity, type 2 diabetes, non-alcoholic fatty liver disease (NAFLD), and cancer[21–24]. Studies have shown that an altered ratio of succinate-producing families, such as *Prevotellaceae* (P) and *Veillonellaceae* (V), to succinate-consuming families, including *Odoribacteraceae* (O) and *Clostridiaceae* (C), is linked to inflammation in various inflammatory conditions[25,26].

SUCNR1 has been shown to be upregulated in inflammatory conditions, while SUCNR1-deficient mice exhibit protection from colitis and intestinal fibrosis[27]. Consistent with this, microbial-derived succinate promotes the release of pro-inflammatory cytokines, including IL-1β, IL-6, IL-8, and TNF-α, which exacerbate inflammation[28–32]. Our previous work demonstrated that succinate stabilizes HIF-1α, which supports the generation and function of IL-9-secreting Th9 cells[17,30]. TGF-β and IL-4 drive the differentiation of naïve $CD4^+$ T cells into Th9 cells through transcription factors such as PU.1, BATF, IRF-1, and Foxo1[33,34]. Th9 cells have been implicated in driving colonic inflammation in experimental colitis through IL-9R-sensitive intestinal epithelial cells[35–37]. SUCNR1-deficient mice exhibit lower IL-9 expression in visceral adipose tissue, suggesting a role of the succinate-SUCNR1 axis in the generation and function of Th9 cells[38]. While the role of succinate and SUCNR1 in pathogenic Th17 cells in arthritis has been established[39,40], their involvement in the generation of colitogenic T cells in ulcerative colitis (UC) remains unclear. Although a few studies have identified sources of succinate contributing to colonic inflammation in UC[14], none have yet investigated the link between microbiota-derived succinate and Th9 cells in the pathogenesis of UC.

In this study, we demonstrate that colitogenic Th9 cells are generated through the succinate-SUCNR1 axis in the oxazolone-induced colitis model. Blocking either IL-9 or SUCNR1 reduces susceptibility to experimental colitis. Furthermore, we identify gut microbiota-derived succinate as a key contributor to tissue inflammation in colitis. We show that dysbiosis associated with colitis leads to an imbalance between succinate-producing and succinate-consuming gut microbiota, promoting succinate production and the generation of colitogenic Th9 cells. Importantly, we demonstrate that colonizing mice with succinate-consuming bacterial consortia or inhibiting SUCNR1 can prevent Th9 cell-mediated immunopathogenesis in Oxa-colitis. Our findings reveal the crucial role of succinate produced by the gut microbiome in the pathogenesis of Th9-driven inflammation during IBD.

Results

Elevated succinate levels correlate with increased disease severity in colitis

In addition to Th2 cells, IL-9-producing Th9 cells play a critical role in the pathogenesis of Oxa-colitis[36]. Neutralizing IL-9 with an anti-IL-9 antibody alleviates the signs of Oxa-colitis, leading to recovery in weight loss and reduction in colonic lesions (Supplementary Fig. 1A–E). Gene profiling data from lamina propria cells of the colon in anti-IL-9-treated mice, compared to untreated mice, showed downregulation of Th9-associated genes (Foxo1, PU.1, GATA-3, BATF, IRF-4, Hif-1α, IL-5, IL-9, IL-33, and IL-21), which are involved in Th9 differentiation and function. This suggests that colitogenic IL-9-producing T cells contribute to colonic inflammation in Oxa-colitis (Supplementary Fig. 1F, G).

To elucidate the molecular mechanisms driving colonic inflammation in Oxa-colitis, we identified metabolites that are differentially modulated in the stool and serum of healthy and Oxa-colitis mice using LC–MS-based untargeted metabolomics. Principal component analysis (PCA) and hierarchical clustering of data revealed distinct patterns of differentially modulated metabolites between the healthy and Oxa-colitis groups (Fig. 1A, B and Supplementary Fig. 1H–K). Among these, we identified several common metabolites that enriched in both stool and serum of Oxa-colitis groups (Supplementary Fig. 1L, M). To validate these findings in human settings, we analysed metabolites in stool and serum samples from healthy volunteers and active UC patients (Fig. 1C, D and Supplementary Fig. 1N–U). By combining the enriched metabolites from Oxa-colitis mice with those from UC patients, we identified succinate as a common metabolite enriched in stool and serum samples from both active UC patients and Oxa-colitis (Fig. 1E).

To investigate the role of succinate and its receptor, SUCNR1, in colitogenic T cell generation and function in the pathogenesis of UC, we assessed the differential expression of SUCNR1 on $CD4^+$T cells from the lamina propria of colons in healthy or Oxa-colitis mice. qPCR data indicated the higher expression of SUCNR1 on $CD4^+$T cells isolated from the lamina propria of the inflamed colon of Oxa-colitis compared to those from the healthy control mice (Supplementary Fig. 2A, B). We observed an increased frequency of $SUCNR1^+$ $CD4^+$ T and $SUCNR1^+$ $IL\text{-}9^+$ $CD4^+$ T cells in the lamina propria of colons from Oxa-colitis mice compared to healthy control mice (Fig. 1F). Consistent with this, we found elevated expression of SUCNR1 on Th2 and Th9 cells, while Th1, Th17, and iTregs did not express SUCNR1 (Supplementary Fig. 1C). These findings align with previous studies showing that both Th2 and Th9 cells are the effector T cell subsets that promote inflammation in Oxa-colitis[36,41].

To directly investigate the role of succinate in driving colonic inflammation in Oxa-colitis, we administered exogenous succinate in drinking water to Oxa-colitis mice and compared them with untreated Oxa-colitis mice. Although exogenous succinate in drinking water failed to elevate fecal succinate levels, it did increase serum succinate levels (Supplementary Fig. 2D–F). However, it did not exacerbate Oxa-colitis or colonic inflammation, as evidenced by no significant body weight reduction, histopathological scoring, and the increase in Th9-associated genes, compared to untreated Oxa-colitis mice (Supplementary Fig. 2G–I). This aligns with previous studies suggesting that a systemic increase in succinate may not be sufficient to induce colonic inflammation in DSS colitis[42,43], highlighting that the local accumulation of succinate within the colon may play a critical role in exacerbating colonic inflammation in Oxa-colitis[42]. We employed polyethylene glycol-3350 (PEG-3350), a safe, palatable, and weight-neutral gastric motility enhancer (Supplementary Fig. 3A, B), to facilitate the accumulation of colonic succinate, as previously described[44] in order to assess its impact on Oxa-colitis (Supplementary Fig. 3C). PEG-3350 treatment exacerbated the severity of Oxa-colitis in mice, as evidenced by enhanced weight loss, colonic lesions, and histopathological scores of inflammations, infiltration, edema, and ulceration, all associated with elevated colonic succinate levels (Supplementary Fig. 3D–H). Additionally, PEG-3350 treated mice exhibited a higher frequency of Th9 cells without increasing the frequency of Th2 cells in the lamina propria of the colon compared to untreated controls (Supplementary Fig. 3I), ruling out the involvement of Th2 cells, which are major producers of IL-4 and known to promote inflammation in Oxa-colitis[41,45]. The increased frequency of Th9 cells in PEG-3350-treated Oxa-colitis mice was correlated with the upregulation of Th9 cell-associated genes (IL-9, Foxo1, and IL-9R), as well as SUNCR1, in T cells isolated from lamina propria of the colon (Supplementary Fig. 3J, K). Additionally, we administered fructo-oligosaccharide (FOS) to elevate colonic and fecal succinate, as previously reported[42,44,46], in order to assess its impact on colonic inflammation in Oxa-colitis. FOS treatment exacerbated colonic inflammation in Oxa-colitis compared to untreated mice, with significantly increased colonic lesions, intestinal inflammation, an increased frequency of Th9 cells, and upregulation of Th9-associated genes (IL-9, IL-9R, IRF-4, PU.1, and Foxo1), along with SUCNR1 (Supplementary Fig. 3L–S). More importantly, FOS treatment, compared to untreated mice, increased colonic succinate levels (Supplementary Fig. 3T). Furthermore, we administered succinate locally to the colon through a succinate-enriched enema to evaluate its direct impact on disease progression in Oxa-colitis (Supplementary Fig. 3U). This treatment aggravated colonic inflammation compared to the untreated group, resulting in significant weight loss, increased colonic lesions, and higher histopathological scores, indicating more severe intestinal inflammation (Supplementary Fig. 3V–X). Consistent with these findings, we detected elevated expression of IL-9 and SUCNR1 genes in the helper T cells isolated from the lamina

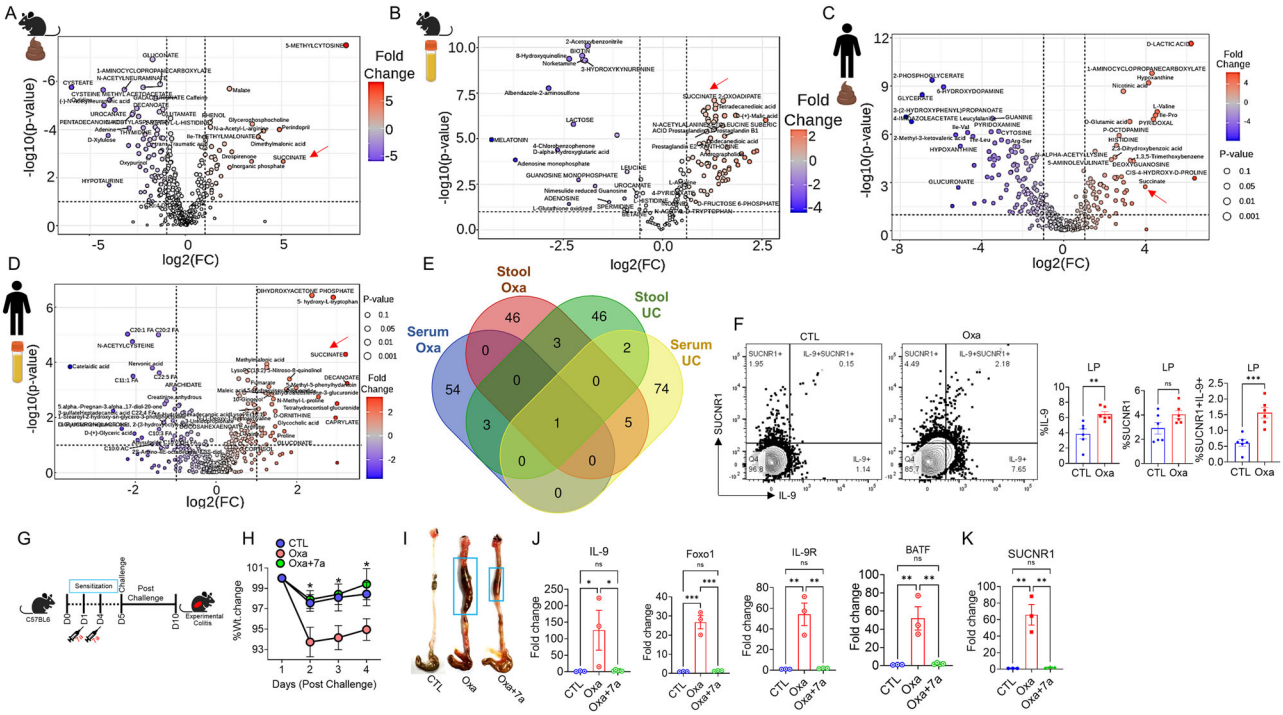

Fig. 1 | Colitis mice and UC patients displayed elevated succinate levels. Treatment with a succinate receptor (SUCNR1) inhibitor in mice led to a decrease in inflammation. A Volcano plots showing differential stool metabolites comparing colitis with healthy controls. **B** Volcano plots showing differential serum metabolites comparing colitis with healthy controls. **C**, **D** Volcano plots showing differential stool and serum metabolites comparing UC with healthy volunteers. **E** The hallmark metabolite, succinate, was significantly upregulated in both the stool and serum compartments of colitis mice and UC patients. The numbers represent various metabolites, with only succinate consistently elevated across all samples. **F** FACS data showing an increased frequency of SUCNR1$^+$ IL-9$^+$ CD4$^+$ T cells in the lamina propria of Oxazolone-colitis mice compared to healthy mice. **G** Schematic illustrating the treatment regimen for SUCNR1 inhibition in oxazolone-induced colitis mice, using compound 7a. **H** Body weight recovery in oxazolone-induced colitis mice treated with compound 7a surpassed that of untreated mice. **I** Inflammatory lesion formation was significantly suppressed in oxazolone-induced colitis mice treated with compound 7a compared to untreated mice. **J** The expression levels of Th9-associated genes, including IL-9, Foxo1, IL-9R, and BATF, were quantified using qPCR from the MLNs of mice treated with compound 7a compared to untreated mice. **K** The expression level of SUCNR1, a surrogate indicator for succinate availability, was measured using qPCR in the MLNs of mice treated with compound 7a compared to untreated mice. $^*P < 0.05$, $^{**}P < 0.01$, $^{***}P < 0.001$, and $^{****}P < 0.0001$ (Student's *t*-test or one-way ANOVA).

propria of these animals (Supplementary Fig. 3Y, Z). Taken together, these results further reinforce the link between colonic succinate and Th9 cells in the context of colonic inflammation.

Blocking of succinate/SUCNR1 axis reduces intestinal inflammation in mice

To confirm the role of succinate and SUCNR1 in driving intestinal inflammation in Oxa-colitis, we utilized SUCNR1 antagonist 7a to block SUCNR1 signaling and function. Previous studies have demonstrated that SUCNR1 antagonist 7a alleviated periodontitis with a notable reduction in average alveolar bone loss[32]. Accordingly, we synthesized SUCNR1 antagonist 7a (Supplementary Fig. 4A–D) and evaluated its impact on inflammatory response in Oxa-colitis. Treatment with 7a significantly reduced the severity of colonic inflammation in Oxa-colitis mice compared to controls, leading to mark improvements in body weight loss, colonic lesions (Fig. 1 G, J), and histopathological scores of inflammation, edema, infiltration, and ulceration (Supplementary Fig. 4E). Consistently, treatment with SUCNR1 antagonist 7a reduced the expression of Th9 cells associated genes, IL-9, IL-9R, FOXO1, BATF, and succinate sensing receptor SUCNR1 (Fig. 1J, K).

To confirm whether SUCNR1 antagonist 7a blocks Th9 cell differentiation, we generated Th9 cells in vitro under Th9 cell differentiating conditions with various doses of SUCNR1 antagonist 7a. Our results demonstrated that SUCNR1 antagonist 7a inhibited Th9 cell differentiation in a dose-dependent manner (Supplementary Fig. 4F). We identified an optimal dose of 7a that maximally suppressed IL-9 production under in vitro differentiated Th9 cells treated with succinate (Supplementary Fig. 4G, H). Additionally, we assessed Th9 cell differentiation across physiological and pathophysiological concentrations of succinate with or without SUCNR1 agonist 7a[14,27,47–49], Our findings revealed that 7a effectively inhibited SUCNR1 activity across the entire range of succinate concentrations (Supplementary Fig. 4I). To further explore the immunological specificity of succinate, we differentiate various T helper cell subsets (Th1, Th2, and Th17) in vitro, both with and without succinate treatment. Unlike Th9 cells, which showed an increase in IL-9 production in response to succinate, other subsets exhibited no significant changes in their respective signature cytokines (Supplementary Fig. 4J).

To understand the molecular mechanism as to how extracellular succinate promotes Th9 cells generation and functions, we assessed HIF-1α expression in these cells. Previous studies have demonstrated that both intracellular and extracellular succinate promote HIF-1α-mediated functions. Intracellular succinate stabilizes HIF-1α by inhibiting the prolyl hydroxylase domain (PHD) enzyme, which is responsible for HIF-1α degradation[17,18], thereby enhancing Th9 cells generation. In contrast, extracellular succinate increases HIF-1α expression through activating its receptor SUCNR1[50–52]. Th9 cells differentiated in the presence of extracellular succinate exhibited elevated HIF-1α expression (Supplementary Fig. 4K). Notably, SUCNR1 antagonist 7a completely abrogated HIF-1α and IL-9 expression in Th9 cells, confirming the role of SUCNR1 signaling in HIF-1α-mediated induction of Th9 cells. Collectively, these findings suggest that succinate, derived from either intracellular or extracellular sources, promotes HIF-1α stabilization through distinct mechanisms. Specifically, extracellular succinate modulates Th9 cells via the succinate-

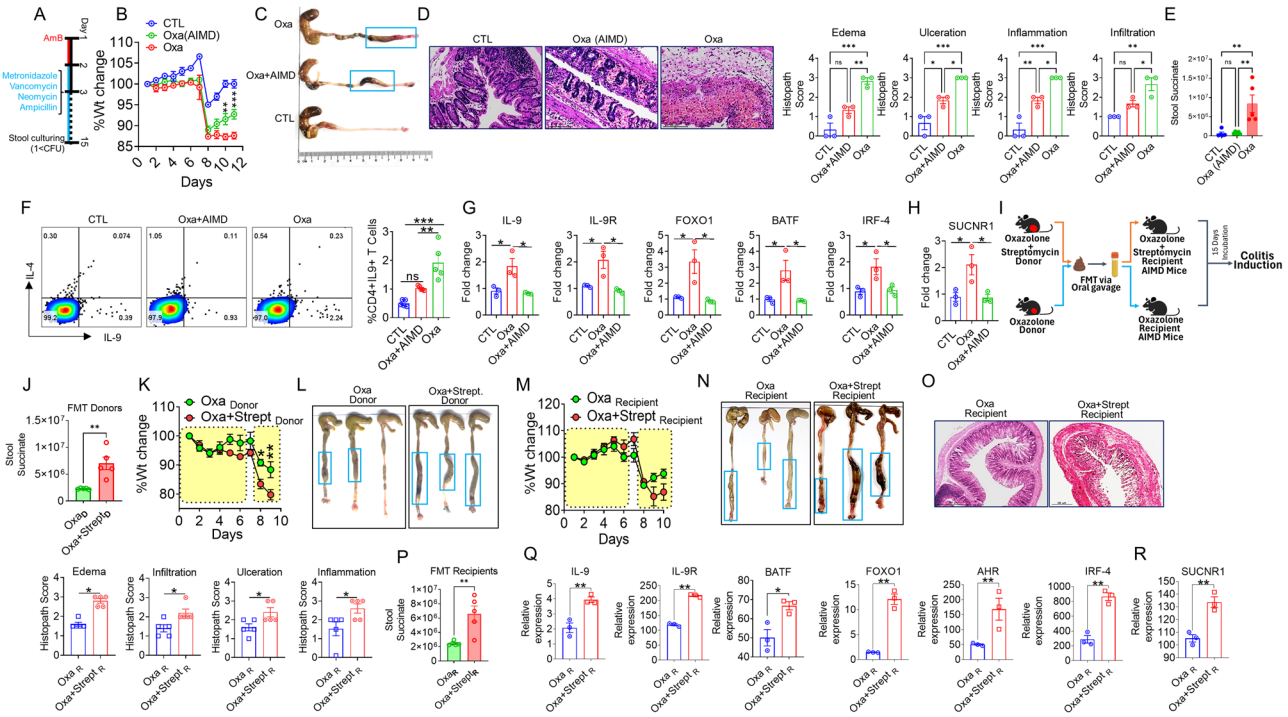

Fig. 2 | The colon tissue-resident microbiota triggers succinate-mediated pro-inflammatory responses in mice with oxazolone-induced colitis. A Schematic of mouse gut microbiome depletion using an antibiotic cocktail [amphotericin-B (0.1 mg/ml; Sigma), ampicillin (1 g/l; Sigma), vancomycin (5 mg/ml; Sigma), metronidazole (10 mg/ml; Sigma), and neomycin (10 mg/ml; Sigma)]. **B** Body weight reduction is less pronounced in AIMD mice than in wild-type mice following colitis induction with oxazolone. **C** Inflammatory lesion formation is significantly suppressed in AIMD mice compared to wild-type mice after colitis induction. **D** Representative hematoxylin and eosin-stained sections of mouse colon tissue, accompanied by blinded histologic scores (scale bar: 100 µm). **E** Fecal succinate levels measured in various groups of animals. **F** Flow cytometry plots of $CD4^{+}IL\text{-}9^{+}$ helper T cells from the colonic lamina propria, along with percentages. **G** The expression levels of Th9-associated genes, including IL-9, Foxo1, IL-9R, and BATF, were quantified using qPCR from the MLNs of treated mice. **H** The expression level of SUCNR1, a surrogate indicator of succinate availability, was measured using qPCR in the MLNs of treated mice. **I** Schematic of fecal succinate elevation using FMT from diseased and streptomycin donors (a concentration of 20 mg in 200 µl of PBS by gavage per mouse for 72 h, followed by colitis induction using oxazolone). **J** Succinate levels measured in stools from diseased and streptomycin-donor mice. **K** Body weight reduction in FMT donors. **L** Inflammatory lesion formation in FMT donors. **M** Body weight reduction in FMT recipients. **N** Inflammatory lesion formation in stool recipients from oxazolone donors and oxazolone-streptomycin-donors. **O** Representative hematoxylin and eosin-stained sections of mouse colon tissue from recipients of oxazolone and oxazolone-streptomycin stools, accompanied by blinded histologic scores. **P** Succinate levels were measured in the stools of recipients of oxazolone and oxazolone-streptomycin stools. **Q** The expression levels of Th9-associated genes, including IL-9, Foxo1, IL-9R, BATF, AHR, and IRF-4, were quantified using qPCR from the MLNs of recipients of oxazolone and oxazolone-streptomycin stools. **R** The expression level of SUCNR1, a surrogate indicator of succinate availability, was measured using qPCR in the MLNs of recipients of oxazolone and oxazolone-streptomycin stools. $^{*}P < 0.05$, $^{**}P < 0.01$, $^{***}P < 0.001$, and $^{****}P < 0.0001$ (Student's *t*-test, one-way ANOVA, or two-way ANOVA).

SUCNR1-HIF-1α axis. These data underscore that succinate-driven colonic inflammation in Oxa-colitis is microbiota-dependent.

The colonic microbiota triggers succinate-mediated pro-inflammatory responses in oxazolone-colitis

Since both cellular respiration and gut commensals contribute to succinate production[12], we sought to identify the source of succinate driving in colonic inflammation in Oxa-colitis. Our analysis revealed elevated succinate levels in fecal samples of Oxa-colitis mice compared to controls, suggesting a link between gut microbiota-derived succinate and colonic inflammation in Oxa-colitis. To investigate this further, we utilized antibiotic-induced microbiome-depleted (AIMD) mice, in which gut microbiota is depleted through a cocktail of antibiotics as previously described[53]. We induced Oxa-colitis in AIMD mice to assess the role of gut microbiota and gut microbiota-derived succinate in intestinal inflammation (Fig. 2A). AIMD mice remained susceptible to Oxa-colitis but exhibited attenuated inflammation, as evidenced by reduced body weight loss and lower histopathological scores of inflammation, edema, infiltration, and ulceration (Fig. 2B–D). Notably, AIMD mice, unlike wild-type mice, did not exhibit an increase in colonic succinate following oxazolone-induced colitis (Fig. 2E). Consistent with these findings, AIMD mice displayed reduced Th9 cell frequency and lower expression of Th9-associated genes (IL-9R, Foxo1, BATF, and IRF-4) as compared to wild-type mice with Oxa-colitis (Fig. 2F–H).

To further confirm the role of gut microbiota-derived succinate in the severity of Oxa-colitis, we conducted a fecal microbiota transplantation (FMT) experiment. Fecal material from two distinct donor groups-Oxa-colitis mice (diseased-donor) and Oxa-colitis mice administered with streptomycin (Streptomycin-donors) was transplanted into AIMD mice (Fig. 2I). Previous studies as well as our findings indicated that the streptomycin administration of modulate the microbiota and promotes succinate production (Fig. 2J–L)[44].

After FMT, recipient AIMD mice were maintained for 15 days before being subjected to an oxazolone challenge to induce Oxa-colitis. FMT from streptomycin-donors compared to diseased-donors, significantly exacerbated the severity of Oxa-colitis, as evidenced by greater body weight loss, more extensive colonic lesions, and higher histopathological scores, including inflammation, cellular infiltration, edema, and ulceration in the colon tissues (Fig. 2M–O). Additionally, fecal succinate levels were markedly elevated (Fig. 2P).

Furthermore, recipient mice that received FMT from streptomycin-donors showed increased expression of SUCNR1 and Th9 cell-associated genes, including IL-9, IL-9R, IRF-4, BATF, and IRF-1, compared to the recipients of FMT from diseased-donors (Fig. 2Q, R). However, no significant changes were observed in the expression of IFN-γ, IL-17, or the frequency of Foxp3+ Tregs (Supplementary Fig. 5A, B). These results underscore the critical role of gut microbiota in driving colonic inflammation in Oxa-colitis.

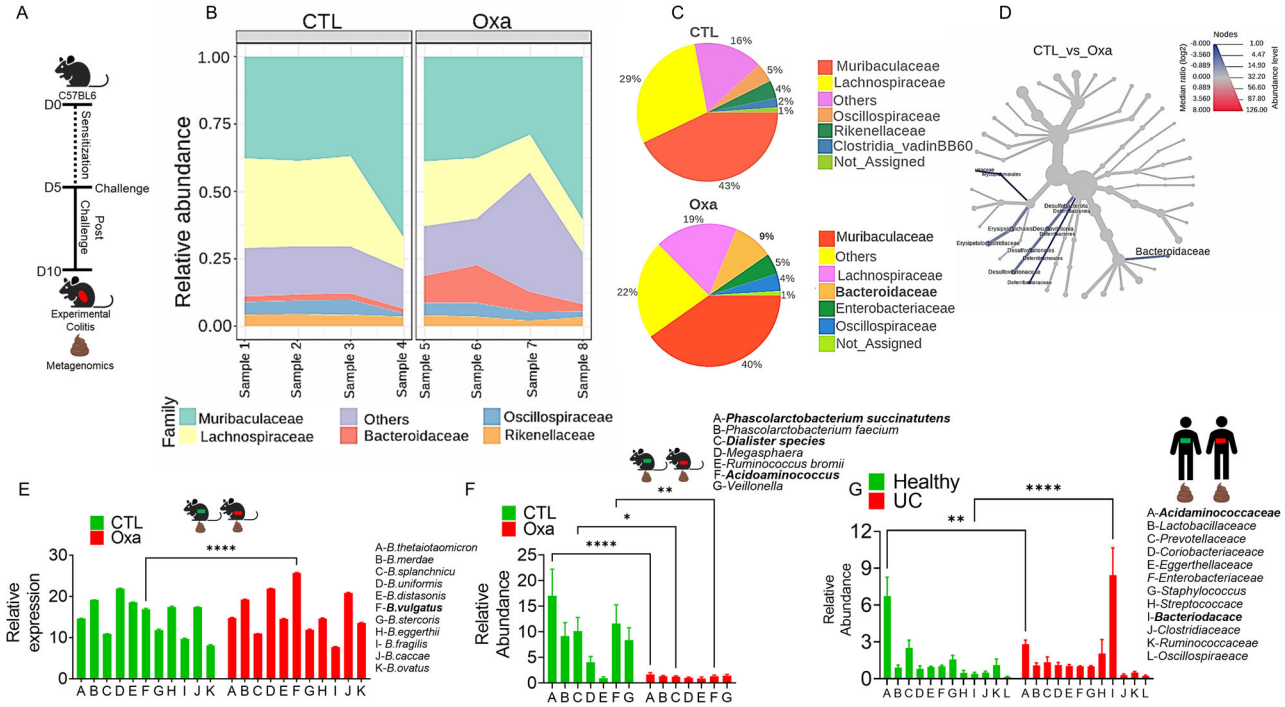

Fig. 3 | Ulcerative colitis disrupts the balance of gut microbes involved in succinate production and metabolism in both humans and mice. A Schematic of stool specimen collection for metagenomics and qPCR. **B** Heatmap showing the top ten microbiota families with their respective relative abundances ($n = 4$). *Bacteroidaceae* was abundant in the Oxa-colitis group compared to the other families. **C** Venn diagram showing the relative abundance (%) of top families between healthy controls and Oxa-colitis. **D** Heat tree analysis depicting alterations in microbiota composition between healthy controls and Oxa-colitis. Significantly altered taxa are displayed by name at the corresponding node. Nodes indicate the hierarchical structure of taxa. A blue branch indicates a decrease in healthy controls compared to Oxa-colitis. **E** Relative abundance of individual species of the *Bacteroidaceae* family in stool specimens collected from healthy controls and the Oxa-colitis group. **F** Relative abundance of individual species of the *Acidaminococcaceae* family in stool specimens collected from healthy controls and the Oxa-colitis group. **G** Compared to healthy individuals, UC patients have a significant increase in the abundance of *Bacteroidaceae*, the major producers of succinate in the gut microbiota, and a decrease in *Acidaminococcaceae*, which is important for succinate metabolism. $^{*}P < 0.05$, $^{**}P < 0.01$, $^{***}P < 0.001$, and $^{****}P < 0.0001$ (One-way ANOVA or two-way ANOVA).

Ulcerative colitis disrupts the balance of gut microbial ecosystem involved in succinate production and metabolism in humans and mice

To identify gut commensals contributing to succinate-mediated aggravation in Oxa-colitis, we performed 16S rRNA sequencing of stool samples from Oxa-colitis and healthy control mice (Fig. 3A). The analysis revealed a selective enrichment of succinate-producing families, notably *Bacteroidaceae*, in Oxa-colitis compared to healthy control (Fig. 3B). Within the *Bacteroidaceae* family *Bacteroides vulgatus* was most predominantly increased followed by *Bacteroides stercoris*, *Bacteroides caccae*, and *Bacteroides ovatus*, ranking among the top ten efficient succinate producers in the gut (Fig. 3C–E).

In contrast, the abundance of central succinate-consuming family *Acidaminococcaceae* was significantly reduced in Oxa-colitis compared to controls. The Species-level analysis showed a marked decrease in *Phascolarctobacterium succinatutens, Dialister species*, and *Acidaminococcus* within the *Acidaminococcaceae* family (Fig. 3F).

We further compared these findings with stool samples from UC patients to assess the microbial abundance at the family level. Consistently with experimental colitis data, UC patients exhibited a significant increase in the succinate-producing family *Bacteroidaceae*[12,14] and a substantial decrease in the succinate-consuming family *Acidaminococcaceae*[12,14] (Fig. 3G). Together, these data highlight an enrichment of succinate-producing gut commensals and a reduction in succinate consumers, linking microbial imbalances to UC pathogenesis.

Colonization with *Bacteroides vulgatus* elevates fecal succinate, promotes IL-9-secreting CD4^{+} T cells, and aggravates oxazolone-colitis

To confirm the role of succinate-producing gut bacteria in exacerbating colonic inflammation in Oxa-colitis, purified *Bacteroides vulgatus* (JCM 5826)was cultured on Bacteroides Bile Esculin (BBE) agar (Supplementary Fig. 5C), and gavaged to AIMD mice, followed by an oxazolone challenge to induce colitis (Fig. 4A, B and Supplementary Fig. 5D). Mice gavaged with *Bacteroides vulgatus* exhibited increased stool succinate levels and signs of aggravated colitis (Fig. 4C), including body weight loss, increased colonic-lesions sizes, and histopathological scores of inflammation, cellular infiltration, edema, and ulceration (Fig. 4D, E). Furthermore, the frequency of Th9 cells and the expression of SUCNR1, IL-9, IL-9R, Foxo1, IRF-4, and BATF were elevated in these mice (Fig. 4F–H).

To access the role of IL-9 and succinate in *B. vulgatus*-mediated colonic inflammation, we used an IL-9 neutralizing antibody or the SUCNR1 antagonist 7a (Fig. 4I). Both treatments suppressed enhanced colitis by preventing weight loss, reducing colonic lesions, and improving histopathological scores (Fig. 4J-L). Additionally, IL-9 neutralization and SUCNR1 blockade led to reduced expression of SUCNR1 and Th9 cell-associated genes (Fig. 4M, N).

Supplementation with retinoic acid disrupts the colonization of *Bacteroides vulgatus*, thereby alleviating Oxa-colitis by reducing fecal succinate levels

Based on the previous findings that *Bacteroides vulgatus* has a retinol sensor which affects its fitness through the bacterial AcrAB-TolC efflux system

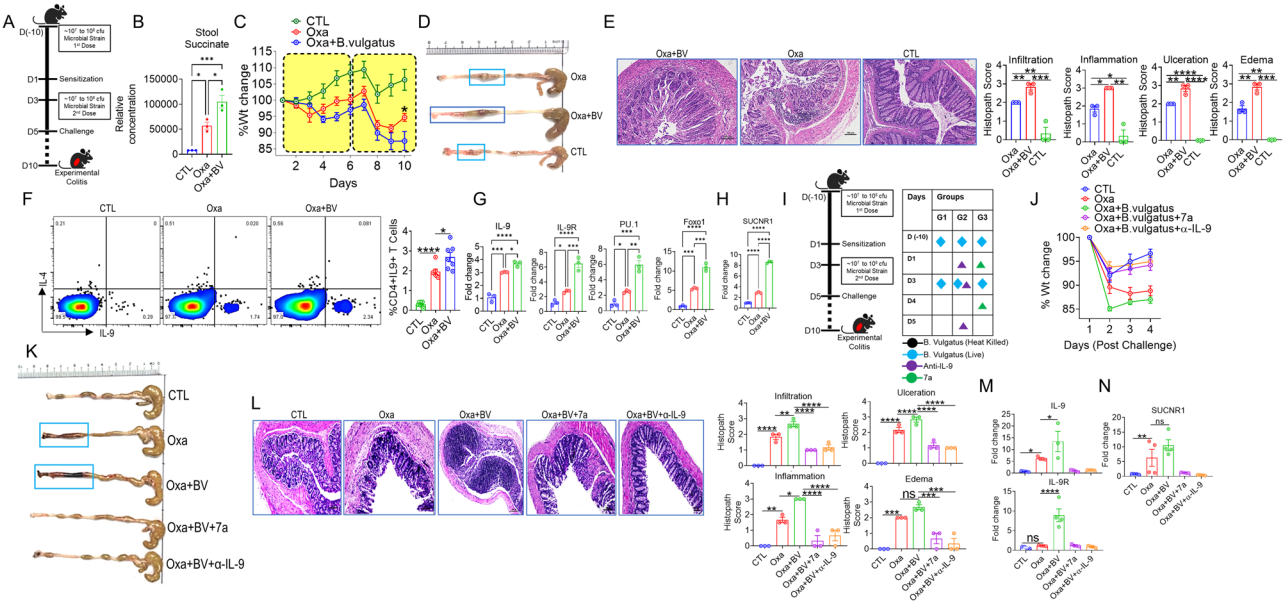

Fig. 4 | Colonization of *Bacteroides vulgatus* increases IL-9-secreting CD4$^+$ T cells and exacerbates oxazolone-colitis due to an elevation in fecal succinate. **A** Schematic of *Bacteroides vulgatus* colonization and colitis induction. **B** Fecal succinate measurement using LC–MS in healthy controls, Oxa alone, and Oxa-colonized with *Bacteroides vulgatus*. **C** Body weight recovery in healthy controls, Oxa alone, and Oxa-colonized with *Bacteroides vulgatus* ($n = 6$). **D** Formation of colonic lesions in healthy controls, Oxa alone, and Oxa-colonized with *Bacteroides vulgatus* ($n = 6$). **E** Representative images of distal colons stained with H&E and respective statistics for pathology scores. **F** Representative FACS plot for IL-9 measurement in helper T cells harvested from the mesentery of healthy controls, oxazolone-treated mice, and Oxa-colonized with *Bacteroides vulgatus* ($n = 6$). **G** Representative qPCR data for the expression of IL-9 and related genes Foxo1, PU.1, and IL-9R. **H** The expression level of SUCNR1, a surrogate indicator for succinate availability, was measured using qPCR in the MLNs of healthy controls, Oxa alone, and Oxa-colonized with Bacteroides vulgatus. **I** Schematic showing colonization of *Bacteroides vulgatus* followed by anti-IL-9 and SUCNR1 antagonist (7a) treatment. **J** Reduction in body weight in healthy controls, Oxa alone, Oxa-colonized with *Bacteroides vulgatus*, Oxa-colonized with *Bacteroides vulgatus* plus 7a, and Oxa-colonized with Bacteroides vulgatus plus anti-IL-9 treatment ($n = 6$). **K** Formation of colonic lesions in healthy controls, Oxa alone, Oxa-colonized with *Bacteroides vulgatus*, Oxa-colonized with *Bacteroides vulgatus* plus 7a, and Oxa-colonized with *Bacteroides vulgatus* plus anti-IL-9 treatment ($n = 6$). **L** Representative images of distal colons stained with H&E and respective statistics for pathology scores of various groups. **M** Representative qPCR data for the expression of IL-9 and associated genes in healthy controls, Oxa alone, Oxa-colonized with *Bacteroides vulgatus*, Oxa-colonized with *Bacteroides vulgatus* plus 7a, and Oxa-colonized with Bacteroides vulgatus plus anti-IL-9 treatment ($n = 6$). **N** The expression level of SUCNR1, a surrogate indicator for succinate availability, was measured using qPCR in the MLNs of healthy controls, Oxa alone, Oxa-colonized with *Bacteroides vulgatus*, Oxa-colonized with *Bacteroides vulgatus* plus 7a, and Oxa-colonized with *Bacteroides vulgatus* plus anti-IL-9 treatment ($n = 6$). $^*P < 0.05$, $^{**}P < 0.01$, $^{***}P < 0.001$, and $^{****}P < 0.0001$ (One-way ANOVA or two-way ANOVA).

upon retinol treatment[54,55]. Previous studies demonstrated vitamin A deficiency enriches *B. vulgatus*, while retinoic acid (RA) supplementation inhibits its growth[54,56].

To investigate whether RA can disrupt *B. vulgatus* colonization and alleviate Oxa-colitis, we gavaged AIMD mice with *B. vulgatus* followed by RA supplementation. RA significantly decreased *B. vulgatus* abundance (Fig. 5A) and ameliorated Oxa-colitis, as shown by prevention of weight loss, reduced colonic lesions, and improved histopathological scores (Fig. 5B–E). RA also reduced the frequency of Th9 cells and the expression of Th9 cell-associated genes, IL-9, Foxo1, IL-9R, IRF-4, GATA-3, and BATF, in T cells from MLNs of Oxa-colitis mice treated with RA, compared to controls (Fig. 5F, G).

To understand the mechanism by which RA inhibits *B.vulgatus*-succinate-mediated inflammation in Oxa-colitis, we analysed the metabolites in stool samples from healthy, Oxa-colitis, and RA-treated Oxa-colitis mice. Principal component analysis (PCA) and hierarchical clustering revealed distinct clusters that effectively differentiated the metabolomic profiles of stool samples from healthy, Oxa-colitis, and RA-treated Oxa-colitis mice (Fig. 5H, I). Among the differentially modulated metabolites in stool samples, a significant decrease in the levels of succinate was found in RA-treated compared to untreated Oxa-colitis mice (Fig. 5J, K), indicating that RA suppresses Oxa-colitis progression by influencing the *B. vulgatus*-succinate axis. Additionally, RA did not significantly affect growth of succinate-metabolizing commensals except for *Dialister succinatiphilus*, which show increased growth in the presence of RA (Supplementary Fig. 5E). These findings support the potential for using RA or RA-producing commensals like *Bifidobacterium bifidum* and *Lactobacillus Intestinalis*, along with succinate-metabolizing gut commensals to treat UC[57].

Succinate-consuming gut bacterial consortium and species protect against oxazolone-induced colitis

To access whether succinate-metabolizing gut commensals and a consortium of commensals can suppress colonic inflammation by limiting succinate availability and inhibiting Th9 cell functions in Oxa-colitis, we colonized AIMD mice with *Phascolarctobacterium succinatutens*, *Dialister succinatiphilus*, and *Dialister propionicifaciens*, and a commensal consortium via oral gavage, followed by a 15-day incubation period. Afterward, the mice were challenged with oxazolone to induce colitis (Fig. 6A). Compared to control mice, those colonize with succinate-metabolizing bacteria or the consortium exhibited protection from Oxa-colitis, as evidenced by reduced body weight loss, absent colonic lesions, and lower histopathological scores and fecal succinate levels (Fig. 6B–G). However, no significant difference in body parameters and pathology were observed in the *Dialister propionicifaciens* group (Supplementary Fig. 5F–I). Additionally, succinate-consuming bacteria and the consortium significantly reduced IL-9-producing Th9 cells and the expression of Th9-related genes such as Foxo1, BATF, and IL-9R, as well as SUCNR1 (Fig. 6H–K). Among these strains, *Dialister succinatiphilus* was selected for further experiments, as it most effectively suppressed colonic inflammation. When co-colonized with *B. vulgatus*, a succinate-producing bacterium, *Dialister succinatiphilus* reduced the *B. vulgatus*-induced enhancement of colonic inflammation in Oxa-colitis mice (Supplementary Fig. 5J). *Dialister succinatiphilus* protection was evident through prevention of body weight loss, absence of colonic

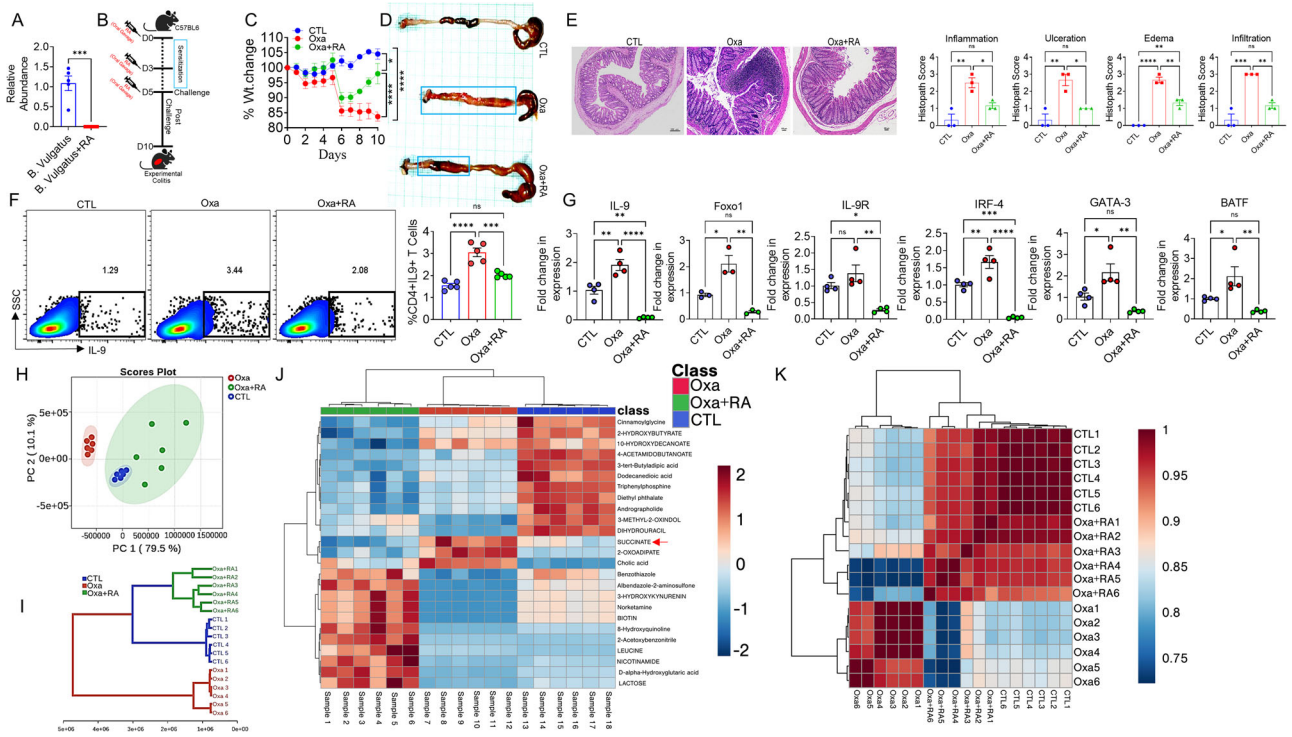

Fig. 5 | Supplementing with retinoic acid disrupts the colonization of *Bacteroides vulgatus*, thereby ameliorating Oxa-colitis through the reduction of fecal succinate levels. **A** Representative qPCR data depicting the relative abundance of *Bacteroides vulgatus* in stool samples from mice with and without retinoic acid (RA) supplementation. **B** Schematic diagram showing the regimen for RA treatment and colitis induction. **C** The reduction in body weight in healthy controls, Oxa alone, and Oxa supplemented with RA. **D** Formation of colonic lesions in healthy controls, Oxa alone, and Oxa supplemented with retinoic acid. **E** Representative images of distal colons stained with H&E, along with respective statistics for pathology scores. **F** Representative FACS plot for IL-9 measurement in helper T cells harvested from the mesentery of healthy controls, Oxa alone, and Oxa supplemented with RA ($n = 6$). **G** Representative qPCR data for the expression of IL-9 and associated genes in healthy controls, Oxa alone, and Oxa supplemented with RA. **H** PCA plot showing distinct metabolic profiles in stool samples collected from healthy controls, Oxa alone, and Oxa supplemented with RA. **I** Hierarchical clustering showing distinct clusters that effectively differentiate the metabolomic profiles of stool samples from healthy, Oxa-colitis, and RA-treated Oxa-colitis mice. **J** The heatmap illustrates stool metabolite analysis from healthy controls, Oxa alone, and Oxa supplemented with RA. Supplemented animals showed a significant reduction in fecal succinate levels. **K** Correlation of identified metabolites with each other. $^{*}P < 0.05$, $^{**}P < 0.01$, $^{***}P < 0.001$, and $^{****}P < 0.0001$ (Student's *t*-test or one-way ANOVA or two-way ANOVA).

lesions, lower histopathological scores, and reduced Th9 cell frequency, as well as decreased expression of SUCNR1, IL-9, IL-9R, Foxo1, and BATF (Supplementary Fig. 5K-O). To further compare the potential of succinate-metabolizing *Dialister succinatiphilus* with IL-9 neutralizing antibody, we tested both interventions in FOS-induced aggravated Oxa-colitis. Both treatments similarly protected FOS-mediated inflammation, as evidenced by the restoration of body weight and a reduction in colonic lesions (Supplementary Fig. 5P–S). Furthermore, treatment reduced $CD4^{+}IL\text{-}9^{+}$ T cell frequency and downregulated SUCNR1 and Th9-associated gene expression (Supplementary Fig. 5T). Finally, the consortium was tested in another colitis model ($CD45RB^{high}$ T cell transfer colitis), where it similarly suppressed inflammation by reducing fecal succinate and $IL\text{-}17^{+}$ $TNF\text{-}\alpha^{+}$ $CD4^{+}$ T cell frequency (Supplementary Fig. 6A–F).

Discussion

In this study, we demonstrate that an imbalance between succinate-producing and succinate-consuming gut bacteria increases colonic succinate availability, which in turn enhances the generation and function of colitogenic T cells, primarily IL-9-producing Th9 cells, through SUCNR1 in ulcerative colitis (UC). UC is characterized by chronic inflammation and ulcers in the innermost lining of the colon. While it was previously believed that Th2 cells played a central role in UC pathogenesis[45], with their effector cytokines IL-5 and IL-13 implicated in colonic inflammation[41,46], recent studies have shifted focus to Th9 cells and their effector cytokine IL-9 as potential therapeutic targets[31,47]. Elevated circulating IL-9 in IBD has been linked to severe prognosis, promoting the formation of pore-forming tight junction protein Claudin-2[49]. Consistent with this, IL-9 and IL-9R have been associated with UC pathogenesis[31], with increased IL-9R expression observed in UC patient gut biopsies[50]. In line with these findings, we show that neutralizing IL-9 with an anti-IL-9 antibody alleviates disease symptoms.

Our findings strongly support the role of succinate in regulating HIF-1α expression and Th9 cell differentiation. As previously reported, intracellular succinate produced during Th9 differentiation stabilizes HIF-1α by inhibiting the PHD enzyme, which is responsible for HIF-1α degradation[17]. In this study, we further demonstrate that extracellular succinate, derived from the gut microbiota, activates the GPR91 receptor, enhancing HIF-1α expression[12,52,58]. The SUCNR1 inhibitor 7a decreased HIF-1α levels, confirming that succinate-mediated activation of the GPR91 receptor is crucial for this effect. These findings not only deepen our understanding of the metabolic regulation of Th9 cells but also suggest that targeting the succinate-SUCNR1-HIF-1α axis could offer therapeutic potential in diseases like IBD, where succinate accumulation is prevalent, as evidenced by a recent study in IBD patients[59].

Disruptions in the intestinal microbiome play a crucial role in the pathogenesis of IBD. Advanced techniques such as metagenomics, metabolomics, and comprehensive immunophenotyping have shed light on alterations in T-cell subsets influenced by microbiota-derived metabolites[51,52]. The present study demonstrates that gut microbiota-derived succinate promotes colitogenic Th9 cells, exacerbating colonic inflammation in UC. This investigation builds on our prior research, where we showed that succinate facilitates Th9 cell differentiation and enhances

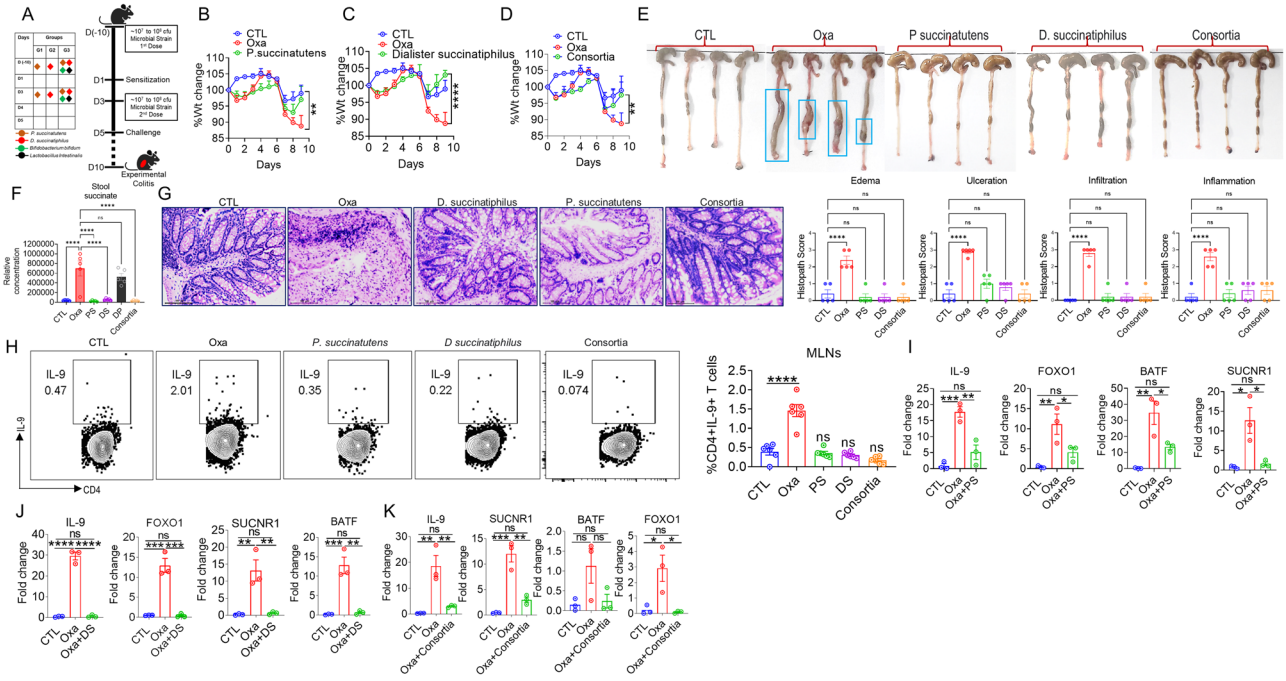

Fig. 6 | The succinate consuming bacterial consortium and individual species protect against oxazolone-induced colitis. A Schematic showing the colonization of the consortium and individual species enriched in succinate consumers. **B** Reduction in body weight of healthy control, Oxa alone, and Oxa-colonized with *Phascolarctobacterium succinatutens* ($n = 6$). **C** Reduction in body weight of healthy control, Oxa alone, and Oxa-colonized with *Dialister succinatiphilus* ($n = 6$). **D** Reduction in body weight of healthy control, Oxa alone, and Oxa-colonized with consortia ($n = 6$). **E** Colonic lesions in Oxa alone, Oxa-colonized with *Phascolarctobacterium succinatutens*, Oxa-colonized with *Dialister succinatiphilus*, and Oxa-colonized with consortia ($n = 6$). **F** Fecal succinate was measured in individual strains and consortia-treated groups of animals. **G** Representative images of distal colons stained with H&E and respective statistics for pathology scores. **H** Representative FACS plot for IL-9 measurement in helper T cells harvested from the mesentery of healthy control, oxazolone, Oxa-colonized with *Phascolarctobacterium succinatutens*, *Oxa-colonized* with *Dialister succinatiphilus*, and Oxa-colonized with consortia. **I**–**K** Representative qPCR data for the expression of IL-9 and associated genes for Th9 and succinate (SUCNR1) in healthy control, Oxa alone, Oxa-colonized with *Phascolarctobacterium succinatutens*, Oxa-colonized with *Dialister succinatiphilus*, and Oxa-colonized with consortia. $^{*}P < 0.05$, $^{**}P < 0.01$, $^{***}P < 0.001$, and $^{****}P < 0.0001$ (one-way ANOVA or two-way ANOVA).

Th9-mediated tumor regression[17]. Our findings indicate that gut dysbiosis associated with UC leads to an accumulation of succinate produced by the microbiota, skewing the gut mucosal immune system toward Th9 cells via the succinate-SUCNR1 axis. The expression of SUCNR1 on these cells was identified as essential for the overproduction of IL-9, contributing to the development of experimental colitis. These results underscore the role of the succinate-SUCNR1 axis in inducing colitogenic Th9 cells and promoting their IL-9 production, exacerbating experimental colitis, in line with previous reports[36]. The observed increase in fecal succinate levels, driven by an imbalance between succinate-producing and metabolizing gut bacterial species, particularly within the *Bacteroidaceae* and *Acidaminococcaceae* families, suggests that this imbalance may persist across various pathophysiological conditions, such as Obesity, Diabetes, Liver fibrosis, NAFLD, Cancer, and Psoriasis, where elevated succinate levels have been detected in serum and stool samples[21,22,26,27,50,51,60].

The approach outlined in this study represents a significant step in understanding the impact of factors such as age, diet, and environmental influences on the Th9 response, which alter microbiota configurations and elevate succinate levels. Although we identified other gut bacterial species that contribute to the skewing of the immune response toward Th9 cells, both our study and that of Serena et al. highlight the potential impact of unbalanced gut microbiota on succinate production and its influence on the host's immune system[26]. This suggests a shared pathway through which various succinate-producing gut microbes modulate this aspect of the host immune response. We further tested the colonization of *Bacteroides vulgatus*, a major succinate-producing bacterial strain, in colitis models to deepen our understanding of microbiota-Th9 crosstalk.

This study exemplifies the significant contributions of the microbiota and its components in shaping host immune responses critical to the development of IBD pathophysiology. We have established a platform to study microbe-host interactions under different physiological and pathological conditions, incorporating methods like fecal material transplantation (FMT), pseudogerm-free mice (AIMD), and selective enrichment of succinate via FOS and PEG-3350 treatment. Additionally, we successfully cultured succinate-metabolizing strains from *Acidaminococcaceae* family and synthesized a selective SUCNR1 blocker, 7a. Finally, our approach for designing a consortium of succinate-metabolizing gut microbes (Indian Patent application No.: 202311037041) has promising therapeutic implications, including the development of next-generation Probiotics and Synbiotics. Furthermore, compound 7a (Cpd-7a) may serve as a potential drug candidate for conditions characterized by elevated succinate levels in serum and stool samples.

Material and methodology

Animals. C57BL/6 (wildtype), antibiotic-induced microbiome-depleted (AIMD), and Foxp3DTR mice (6–8 weeks old) were procured from Jackson Laboratory, housed, and maintained in the small animal facility (SAF) at the Translational Health Science and Technology Institute (THSTI). The mice were kept under the required conditions of a 12-h light/dark cycle with ad libitum chow and water. All animals used for experimental purposes were 6–8 weeks old and were approved by the Institutional Animal Ethics Committee (IAEC) of THSTI, India. The study followed the guidelines outlined by the IAEC of THSTI for conducting research on laboratory animals.

Induction of acute colitis with oxazolone and treatment with anti-IL-9. For the induction of acute colitis by oxazolone, wild-type mice (6 to 8 weeks old) were sensitized by epicutaneous application of 100 µl of 3%

oxazolone (4-ethoxymethylene-2-phenyl-2-oxazolin-5-one; Sigma-Aldrich; #SLCC3834) at a dilution of 4:1 in a mixture of acetone and oil (Olive oil; Del Monte) on day 0. This was followed by intrarectal administration of 100 µl of 1% oxazolone in 50% ethanol (EMSURE® ACS; Merck) on either day 6 or 7. For IL-9 neutralization, wild-type mice were treated intraperitoneally with 40 µg of Anti-IL-9 (Bioxcell) every alternate day, starting before the intrarectal administration.

Induction of acute colitis with oxazolone and treatment with retinoic acid. For the induction of acute colitis by oxazolone, wild-type mice (8 to 10 weeks old) were sensitized by epicutaneous application of 100 µl of 3% oxazolone (4-ethoxymethylene-2-phenyl-2-oxazolin-5-one; Sigma-Aldrich; #SLCC3834) at a dilution of 4:1 in a mixture of acetone and olive oil (Del Monte) on day 0. This was followed by intrarectal administration of 100 µl of 1% oxazolone in 50% ethanol (EMSURE® ACS; Merck) on day 5 using BECTON DICKINSON 427411 Intramedic Semi-Rigid Tubing (0.023" ID, 0.038" OD, PE# 50, Non-Sterile, 1825 days shelf life). For retinoic acid (RA) treatment, mice were given RA in corn oil (450 µg/mouse/time point) orally every other day until the end of the experiment, starting from day 0.

Succinate-enriched enema as an intervention for oxazolone-colitis in mice. Wild-type mice (8 to 10 weeks old) were sensitized by epicutaneous application of 100 µl of 3% oxazolone (4-ethoxymethylene-2-phenyl-2-oxazolin-5-one; Sigma-Aldrich; #SLCC3834), at a dilution of 4:1 in a mixture of acetone and olive oil (Del Monte) on day 0. On day 3, 150 µl of the succinate-enriched enema solution (20 mM) was instilled via the rectum using a 1-mL Luer Lock syringe attached to a 23G needle and lubricated polyethylene tubing (0.048" O.D.). The lubricated tubing was inserted 1 cm into the rectum of isoflurane-anesthetized mice. The enema was administered over a period of 1–2 min to prevent injury. After administration, the tubing was gently removed, and the animals were placed in clean cages to recover. Mice were monitored for any signs of distress or adverse reactions, including gastrointestinal symptoms or changes in behavior, during the course of the experiment. On day 5, the animals were challenged by intrarectal administration of 100 µl of 1% oxazolone in 50% ethanol (EMSURE® ACS; Merck) using Becton Dickinson 427411 Intramedic Semi-Rigid Tubing (0.023" ID, 0.038" OD, PE# 50, non-sterile, 1825 days shelf life).

In vivo imaging of mice. For in vivo imaging of Oxa-colitis mice, the IVIS 100 imaging system (PerkinElmer) was used. This system consists of a sealed chamber equipped with a cooled charge-coupled device (CCD) camera. The chemiluminescent probe luminol (Sigma; #MKBK3960V) was dissolved in water for injection (WFI; Super Amp, 5 ml) and administered intraperitoneally (500 mg/kg) in an injection volume of 100 µl. After 7 min following luminol injection, the bioluminescent signal from the mice's abdomens was detected with a 60-s exposure time. Finally, bioluminescence images were presented as radiance in photon/sec/cm²/sr. During in vivo imaging, the mice were immobilized for the administration of isoflurane. Light emission from the region of interest (ROI) was quantified.

Intracellular cytokine staining and FACS Analysis. Total lymphocytes isolated from the spleen, MLNs, and LNs were re-stimulated with PMA (phorbol 12-myristate 13-acetate; 50 ng/ml; Sigma-Aldrich), ionomycin (1.0 µg/ml; Sigma-Aldrich), and monensin (Golgi Stop, BD Biosciences Cat # 554724) for 5 h. Cell surface staining was performed for 15–20 minutes with anti-mouse CD4 (PerCP)/CD4 (APC) and anti-mouse CD8a (FITC) antibodies after live/dead (Violet fluorescence; Invitrogen by Thermo Fisher Scientific; #1876936) marker staining. For intracellular staining, cells were fixed in Cytofix solution and permeabilized with 1X Perm/Wash Buffer using a kit (BD Biosciences Cat # 554714). The cells were then stained with anti-mouse IL-17 (PE/Cy7), IL-9 (PerCP), IL-10 (APC), IFNγ (PE), IL-4 (PE/Cy7), IRF-4 (PE), and Foxp3 (FITC; APC) antibodies in Perm/Wash buffer. The cells were acquired using flow cytometry on a FACS Canto II with FACS Diva software version 8.0.2 (BD Biosciences) or on a FACS Verse (BD Biosciences), and the results were analyzed with FlowJo software version 10 (Tree Star).

16S rRNA sequencing and metagenomics analysis. Genomic DNA extraction was carried out using the PureLink™ Microbiome DNA Purification Kit (#A29789, Thermo Fisher Scientific) according to the manufacturer's protocol. The samples were processed and analyzed by CoTeRi (NIBMG, India) for 16S rRNA sequencing using barcoded PCR primers targeting the V3-V4 region. Libraries were then prepared for amplicon sequencing using the NEBNext Ultra DNA Library Preparation Kit. These V3-V4 amplicon libraries were quantified and loaded onto the cBot for cluster generation and sequencing. PCR reactions were performed in quadruplicate and pooled for sequencing on the Illumina HiSeq 2500 instrument, yielding 250 bp paired-end sequence reads.

16S rRNA raw reads were quality-controlled using Trimmomatic version 0.39. It removes adapters and trims low-quality bases from the 3′ and 5′ ends of reads to generate decontaminated raw reads, also discarding trimmed reads shorter than 36 nucleotides. A custom pipeline, Quantitative Insights into Microbial Ecology (QIIME2, version 2018.11), was used to process and analyse the decontaminated raw reads. The DADA2 program was used for demultiplexing and joining to generate long sequences. It processes the demultiplexed FASTQ files and produces sequence abundances. Following this, all sequences were grouped into operational taxonomic units (OTUs) using a pretrained Naive Bayes classifier, and their taxonomy was assigned by searching with the Silva ribosomal RNA (rRNA) database (release-138) at 97% sequence similarity.

Alpha diversity indices, including Shannon and Simpson diversity, were computed and plotted using R scripts with the vegan, ape, ggplot2, and phyloseq packages. Differential taxon abundance analysis was also performed using the RAM package in R.

Metabolomics analysis of serum samples using LC–MS/MS: sample preparation, acquisition, data processing, and analysis. A total of 100 µl of serum samples isolated from animals was mixed with LC–MS grade methanol at a 1:3 ratio (serum: methanol), and the clear supernatant was transferred to a sterile LC vial (60 µl/tube). These samples were then kept for drying in a MiVac Duo concentrator (GeneVac Ltd., U.K.). The dried pellet was subsequently dissolved in an 8:2 (v/v) acetonitrile: water mixture for analysis on a chromatography system (Thermo Fisher 5000).

Separation was performed using a UPLC Ultimate 3000 equipped with an HSS T3 column (2.1 × 100 mm, 1.7 µm; Waters Corporation) at 40 °C. The mobile phase was delivered at 300 µl/min and consisted of eluent A (water with 0.1% formic acid) and eluent B (acetonitrile with 0.1% formic acid), following a gradient profile: 0 min—1% B, 1 min—15% B, 4 min—35% B, 7 min—95% B, 9 min— 95% B, 10 min—1% B, 14 min—1% B.

The electrospray ionization (ESI) source was operated in both positive mode (+) and negative mode (−) at 120,000 resolutions in MS1 mode and 30,000 resolutions in data-dependent MS2 scan mode. The spray voltages used for the positive and negative modes were 4000 and 3500 volts, respectively. Sheath gas and auxiliary gas were set to 42 and 11, respectively. The mass scan range was 50–1000 m/z, with an AGC (Automatic Gain Control) target of 200,000 ions and a maximum injection time of 80 ms for MS. For MSMS, the AGC target was set to 20,000 ions, and the maximum injection time was 60 ms.

All acquired LC–MS data were processed using Progenesis QI for Metabolomics (Waters Corporation) software with default settings. The untargeted workflow of Progenesis QI was used for retention time alignment, feature detection, deconvolution, and elemental composition prediction. The Metascope plugin of Progenesis QI was then utilized for an in-house library search, using accurate mass, fragmentation patterns, and retention time. For further validation, an online spectral library was also used. Peaks with a coefficient of variation (CV) of less than 30% in the pool

QC sample were retained for further analysis. Additionally, manual verification of each detected feature was performed to select the correct peaks.

Data analysis was performed using the MetaboAnalyst.ca online tool, which includes normalization, multivariate statistical analysis, and data annotation. Outlier samples were identified and removed by a combination of PCA and random forest, followed by univariate ANOVA analysis.

Metabolomics analysis of stool samples using LC–MS/MS: sample preparation, acquisition, data processing, and analysis. Freeze-dried fecal samples (50 mg of each) were extracted using an extraction solvent composed of methanol and water (1:1). The cells were disrupted using bead beating, sonication, and freeze-thaw lysis methods. The samples were then centrifuged at 13,000×*g* for 15 min, after which the supernatant was transferred to a sterile LC vial (60 µl/tube). These samples were then dried using a MiVac Duo concentrator (GeneVac Ltd., U.K.). The dried pellet was subsequently dissolved in an 8:2 (v/v) acetonitrile: water mixture for analysis on a chromatography system (Thermo Fisher).

Separation was performed using a UPLC Ultimate 3000 system with an HSS T3 column (2.1 × 100 mm, 1.7 µm; Waters Corporation) at 40 °C. The mobile phase was delivered at 300 µL/min and consisted of eluent A (water with 0.1% formic acid) and eluent B (acetonitrile with 0.1% formic acid) in a gradient profile: 0 min—1% B, 1 min—15% B, 4 min—35% B, 7 min—95% B, 9 min—95% B, 10 min—1% B, 14 min—1% B.

The electrospray ionization (ESI) source was operated in both positive mode (+) and negative mode (−) with a resolution of 120,000 in MS1 mode and 30,000 in data-dependent MS2 scan mode. The spray voltage for positive and negative modes was set to 4000 and 3500 volts, respectively. Sheath gas and auxiliary gas were set to 42 and 11, respectively. The mass scan range was 50–1000 m/z, with an AGC (Automatic Gain Control) target of 200,000 ions and a maximum injection time of 80 ms for MS. The AGC target was 20,000 ions, with a maximum injection time of 60 ms for MS/MS.

All acquired LC–MS data were processed using Progenesis QI for metabolomics (Waters Corporation) software with default settings. The untargeted workflow in Progenesis QI was used for retention time alignment, feature detection, deconvolution, and elemental composition prediction. The Metascope plugin of Progenesis QI was then used for in-house library searches based on accurate mass, fragmentation patterns, and retention times. For further validation, an online available spectral library was used. Peaks with a coefficient of variation (CV) of less than 30% in the pooled QC sample were kept for further analysis. Additionally, each detected feature was manually verified to ensure the correct peaks were selected.

Data analysis was performed using the MetaboAnalyst.ca online tool, which involves normalization, multivariate statistical analysis, and data annotation. Outlier samples were identified and removed using a combination of PCA, random forest, and univariate ANOVA analysis.

Quantitative PCR. The RNA extraction from the samples was performed using the RNeasy kit (#74104, Qiagen), and cDNA was synthesized using the iScript cDNA Synthesis Kit (#1708891, Bio-Rad). Quantitative PCR (qPCR) was then conducted using the SYBR Green Gene Expression Assay with the Fast 7500 Dx qPCR system (Applied Biosystems). Ct values for the individual samples (genes) were normalized to the endogenous control (β-Actin/GAPDH) gene expression. All primer sets were purchased from Sigma-Aldrich. The qPCR results were analyzed using SDS 2.1 software. The Ct value of the endogenous control gene was subtracted from the Ct value of each target gene to determine the ΔCT. The relative expression and fold change of each gene were calculated using the following formula: POWER (2, -ΔCT) × 10,000; fold change = 2^−ΔΔCt. All primers used in this study are listed in Supplementary Table 1.

16S rRNA gene quantitative PCR analysis. Bacterial genomic DNA was isolated from mouse fecal pellets or luminal contents using the PureLink™ Microbiome DNA Purification Kit (#A29789, Thermo Fisher Scientific). Quantitative PCR analysis was performed using universal 16S primers to detect all bacterial species and was normalized to the endogenous control (rpoB/recA), dilution, total bacterial amount, and stool sample weight. All primers used in this study are listed in Supplementary Table 2.

GC-MS sample preparation, acquisition, and analysis for short-chain fatty acids (SCFAs). Frozen stool, serum, or colon tissues were resuspended in 0.1% formic acid in NFW and homogenized using a hand homogenizer. Butyrate, propionate, and succinate standards were included in each run to generate standard curves for quantification. The samples were acidified with 12 M HCl, and short-chain fatty acids (SCFAs) were extracted using two cycles of diethyl ether. Each sample was derivatized with N-tert-butyldimethylsilyl-N-methyltrifluoracetamide (MTBSTFA; Sigma-Aldrich) and quantified using a gas chromatograph (Shimadzu; serial number 0217658) coupled to a mass spectrometer detector. Analyses were performed in split mode (1:100) on a DB-5MSUI capillary column (30 m × 0.25 mm, 0.25-µm film thickness, Agilent Technologies), using electron impact ionization (70 eV) and scanning in the m/z range of 50–550. The column head pressure was set to 12 psi. Injector, source, and quadrupole temperatures were 250, 280, and 150 °C, respectively. The GC oven was programmed as follows: 75 °C held for 2 min, increased to 120 °C at 40 °C/min, held at 120 °C for 5 min, increased to 320 °C at 20 °C/min, and held at 320 °C for 7 min.

Culturing of anaerobes. All culture experiments were performed using an anaerobic glove box and a chamber containing an Anaero-Gas pack (Himedia; LE002A-5NO) and MGC oxygen indicator (Ageless Eye). For culturing succinate-consuming bacteria, L-type pure cultures of JCM strains, including *Phascolarctobacterium succinatutens* JCM 16074, *Phascolarctobacterium faecium* JCM 30894, *Dialister succinatiphilus* JCM 15077, and *Dialister propionicifaciens* JCM 17568, were purchased from the Microbe Division (RIKEN BRC; Japan). All four strains were handled in an anaerobic glove box. Among them, *Phascolarctobacterium succinatutens* and *Phascolarctobacterium faecium* were cultured on Columbia blood agar (5% Sheep Blood) plates containing 1% succinate and simultaneously in Tryptic Soy Broth. The remaining two bacteria, *Dialister succinatiphilus* and *Dialister propionicifaciens*, were cultured on Tryptic Soy Blood Agar as well as in Tryptic Soy Broth simultaneously.

For culturing succinate-producing bacteria, mouse stool samples were collected in PBS and cultured on BBE (Bacteroides Bile Esculin) agar containing Gentamicin for the isolation of the *Bacteroides* group of bacteria. For the *Bacteroides vulgatus* gavaging experiment, L-type pure culture of bacteria (*Phocaeicola vulgatus* JCM 5826; Microbe Division; RIKEN BRC; Japan) was grown on BBE agar plates and Tryptic Soy Broth simultaneously. Glycerol stocks of each bacterium were stored at −80 °C for future use.

Bowel cleaning and fecal microbiota transplantation (FMT). After 5 days of cohousing, C57BL/6 mice were given a cocktail of metronidazole (1 g/L), vancomycin (1 g/L), and streptomycin (2 g/L) in drinking water for 4–5 days to deplete the microbiota in the gastrointestinal (GI) tract. FMT was performed through oral gavage, with the first dose consisting of mucus, followed by two doses of feces from donor animals (diseased-donor and streptomycin-donor). Later, the recipient animals were presensitized with 3% oxazolone, followed by an intracolonic challenge with 0.5% oxazolone to induce colitis and compare the disease severity in both groups.

Colonization of succinate-consuming and succinate-producing bacteria and colitis induction experiment. Pure cultures of *Phascolarctobacterium succinatutens* JCM 16074, *Phascolarctobacterium faecium* JCM 30894, *Dialister succinatiphilus* JCM 15077, *Dialister propionicifaciens* JCM 17568, and *Bacteroides vulgatus* JCM 5826 were

used for the colonization experiment. The desired colony-forming units (CFU) (~10^7 to 10^8 CFU/animal) of these strains were calculated based on optical density (OD) measurements (0.4 to 0.5 OD), followed by culturing at different dilutions on their respective agar plates. Once the CFU calculations were completed, the desired CFU of succinate-consuming and succinate-producing bacteria were gavaged into PEG-3350-treated animals. The recipient animals were then presensitized with 3% Oxazolone, followed by an intracolonic challenge with 0.5% Oxazolone to induce colitis. The disease severity in wild-type, succinate-consuming, and succinate-producing bacteria-colonized animals was then compared.

Succinate accumulation in the gut by PEG-3350 treatment. To increase succinate levels in the fecal content, C57BL/6 mice, presensitized with 3% oxazolone, were given 10% PEG-3350 in drinking water for 3 days, followed by an intracolonic challenge with 1% oxazolone to induce colitis.

Succinate accumulation in the gut by fructo-oligosaccharide treatment (FOS). To increase succinate levels in the fecal content, C57BL/6 mice were given 10% FOS in their drinking water for 20 days, followed by sensitization and an intracolonic challenge with 3 and 1% oxazolone to induce colitis.

Oral succinate supplementation. The animals were given 20 mM sodium succinate in their drinking water for 4 weeks, followed by sensitization and intracolonic challenge with 3 and 1% oxazolone to induce colitis, respectively. Oral succinate was administered continuously until the end of the experiment.

Histopathology. The colon was fixed in 10% buffered formalin (Sigma) and processed for hematoxylin and eosin (H&E) staining by the Histopathological service at ILBS Biobank, New Delhi, India. The slides were scored blindly for intestinal inflammation on a scale of 1 to 3, as previously described in the literature.

AIMD mice generation and maintenance. According to the official guidelines and ethics statement, antibiotic-induced microbiome-depleted (AIMD) mice were generated at SAF, THSTI, by administering a cocktail of antibiotics to C57BL/6 mice. The antibiotic regimen began with three days of oral gavage (every 12 h) of amphotericin-B (0.1 mg/ml; Sigma). Starting on day 3, ampicillin (1 g/l; Sigma) was added to the mice's water bottle, and the solution was replaced with a fresh one every third day. A cocktail of vancomycin (5 mg/ml; Sigma), metronidazole (10 mg/ml; Sigma), and neomycin (10 mg/ml; Sigma) was also administered starting on day 3 (oral gavage, every 12 h). The gavage volume for each mouse was 10 ml/kg of body weight. Each animal was kept singly due to its coprophagic behavior. The course of antibiotics continued until depletion was confirmed by stool culture showing <1 cfu.

SUCNR1 antagonist synthesis and characterization. The target compound **cpd-7a** was synthesized by a three-step process as reported in the literature with minor modifications[61,62]. Ethyl bromoacetate on Suzuki coupling reaction with 4-acetylphenylboronic acid in the presence of palladium acetate, tri(o-tolyl) phosphine along with excess potassium phosphate in dry THF resulted in the formation of ethyl 4-acetylphenylacetate **2** which on treatment with 2-aminonicotinaldehyde in the presence of L-proline in ethanol yielded Ethyl 2-(4-(1, 8-napthyridin-2-yl) phenyl) acetate (**3**). The intermediate **3** was then converted to the desired product **cpd-7a** by reaction with methylamine (2 M in THF) in the presence of 1, 8-diazabicyclo [5.4.0] undec-7-ene (DBU).

General. 4-Acetylphenylboronic acid, palladium acetate, tri(o-tolyl) phosphine, L-proline, 2-aminonicotinaldehyde, and methylamine (2 M in THF) were procured from TCI chemicals. Ethyl bromoacetate and DBU were purchased from Avra. The organic solvents were dried by standard procedures wherever necessary. The bulk solvents (hexane, DCM) were distilled before use. All the reactions were monitored by thin layer chromatography (TLC) carried out on Merck silica-gel F254 aluminum sheets and visualized under UV light at 254 and/or 360 nm. The reaction under microwave irradiation was carried out using Synthos 3000 MW reactor by Anton Paar. ^{1}H NMR was recorded on Bruker Advance II 500 MHz in $CDCl_3$, and chemical shifts are reported in parts per million (ppm) relative to tetramethyl silane (TMS) as internal standard. Mass spectrometric analysis was performed with Waters, Q-TOF-Micro mass (ESI-MS) Spectrometer. Purity analysis of the final compound was done using the Agilent 1260 Infinity II High Pressure Liquid Chromatography (HPLC) system.

Scheme 1.

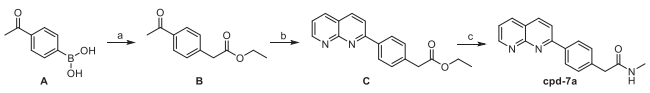

Reagents and Conditions: (a) Ethyl bromoacetate, Pd $(OAc)_2$, $P(o\text{-}tol)_3$, K_3PO_4, THF, 24 h, rt; (b) 2-aminonicotinaldehyde, L-Proline, EtOH, 6 h, 100 °C (microwave); (c) Methylamine (2 M in THF), DBU, 72 h, rt.

Ethyl 2-(4-acetylphenyl) acetate (**B**): A solution of 4-Acetyl phenylboronic acid (1.0 gm, 1.0 eq.) in dry THF (40 mL) was added under inert atmosphere to a solid mixture of palladium acetate (41.0 mg, 3 mol%), tri(o-tolyl) phosphine (167.4 mg, 9 mol%), ethyl bromoacetate (0.8 mL, 1.2 eq.), and excess of potassium phosphate (6.4 gm, 5.0 eq.) in a round bottom flask. The resulting reaction mixture was stirred at room temperature overnight. After the completion of the reaction (monitored through TLC), the reaction mixture was poured on crushed ice, and the product formed was extracted using dichloromethane (3 × 100 mL). The combined organic layer was dried over anhydrous Na_2SO_4, filtered, and evaporated under reduced pressure to obtain the crude product. The crude obtained was further purified using silica-gel (230–400 mesh) column chromatography to obtain compound **2** (758 mg, 60% yield) as a colorless oil. ^{1}H NMR (500 MHz, $CDCl_3$) δ 7.92 (d, J = 8.2 Hz, 2H), 7.39 (d, J = 8.2 Hz, 2H), 4.16 (q, J = 7.1 Hz, 2H), 3.67 (s, 2H), 2.59 (s, 3H), 1.26 (t, J = 7.1 Hz, 3H).

Ethyl 2-(4-(1,8-naphthyridin-2-yl)phenyl) acetate (**C**): Compound **B** (50 mg, 1.0 eq.), 2-aminonicotinaldehyde (27 mg, 1.0 eq), L-proline (28 mg, 1.0 eq.) and ethanol (2 mL) were added in a 5 mL microwave vial and the vial was sealed. The mixture was then heated at 100 °C for 6 h under the microwave irradiation. After the completion of the reaction (monitored by TLC), the reaction mixture was evaporated under reduced pressure to obtain the crude product as a dark brown gel which was then purified using silica-gel (230–400 mesh) column chromatography to get the intermediate compound **C** (13 mg, 19%) as yellow solid. MS (ESI-TOF) *m/z* calculated for $C_{18}H_{16}N_2O_2[M + H]^+$293.1, found 293.3.

2-(4-(1,8-Naphthyridin-2-yl) phenyl)-N-methyl acetamide (**cpd-7a**): Compound **C** (50 mg, 1.0 eq.), DBU (5.1 µL, 0.2 eq.) and methylamine (2 M in THF) (1.0 mL, 10.0 eq.) were added in a 5 mL pressure vessel. The pressure vessel was then sealed, and the reaction mixture was stirred at room temperature for 3 days. After the completion of reaction (monitored through TLC), the reaction mixture was then poured into water (5 mL) and the product obtained was extracted using dichloromethane (3 × 10 mL). The combined organic layer was dried using anhydrous Na_2SO_4, filtered, and evaporated under reduced pressure to obtain the crude product. The crude obtained was then purified using silica-gel (230–400 mesh) column chromatography to get the desired **cpd-7a** (22 mg, 46.8%, 98.75% purity). ^{1}H NMR (500 MHz, CDCl3) δ 9.15 (dd, J = 4.2, 2.0 Hz, 1H), 8.33 – 8.31 (m, 2H), 8.28 (d, J = 8.5 Hz, 1H), 8.22 (dd, J = 8.1, 2.0 Hz, 1H), 8.02 (d, J = 8.5 Hz, 1H), 7.50 (dd, J = 8.1, 4.2 Hz, 1H), 7.44 (d, J = 8.3 Hz, 2H), 3.67 (s, 2H), 2.79 (d, J = 4.9 Hz, 3H); MS (ESI-TOF) *m/z* calculated for $C_{17}H_{15}N_3O$ $[M + H]_+$278.1, found 278.1.

In vitro evaluation of antagonistic properties of SUCNR1 antagonist. Naïve $CD4^+$ ($CD62L^+$ $CD44^-$ $CD25^-$ $CD4^+$) T cells were sorted from the spleens and the lymph nodes of C57BL/6 mice. Naïve $CD4^+$ T cells (100,000 cells) were seeded in a flat bottom 96-well plate precoated with anti-CD3 (0.25 µg/mL) and anti-CD28 (1 µg/mL anti-CD28) in T cell medium (IMDM, 10% fetal bovine serum, 25 mM glutamine, 55 µM 2-mercaptoethanol, 100 U/mL penicillin, and 100 mg/mL streptomycin). For Th9 cell differentiation, T cells were cultured with 10 ng/mL of IL-4 and 0.5 ng/mL of TGF-β with or without SUCNR1 antagonist, 7a, in different doses (50, 25, and 12.5 µM).

In vivo testing of SUCNR1 antagonist and colitis severity. For testing the effect of selective SUCNR1 antagonist, 7a, in the acute colitis induced by oxazolone, wild-type mice (6 to 8 weeks) were sensitized by epicutaneous application 100 µl of 3% of oxazolone (4-ethoxymethylene-2-phenyl-2-Oxazolin-5-one; Sigma-Aldrich; #SLCC3834) at a dilution of 4:1 in a mixture of acetone and oil (Olive oil; Del Monte) on day 0, followed by intrarectal (BECTON DICKINSON 427411 Intramedic Semi-Rigid Tubing, 0.023" ID, 0.038" OD, PE# 50, Non-Sterile, 1825 Days Shelf Life) administration of 100 µl (7 mg/ml Stock) of SUCNR1 antagonist, 7a, on day 4 and day 6. Intracolonic challenge using 0.5% oxazolone in 50% ethanol (EMSURE® ACS; Merck) was performed in the sensitized animals on day 5.

Quantification of succinate in human stool samples. Succinic acid (SA) was analysed using a highly selective MRM method, whilst deuterated form D4-acetic acid was used as an internal standard. SA analysis was performed using Shimadzu GCMS TQ8050NX (S. No. 0217658), and samples were directly injected using an AOC20i injector. The run time of the GC method was 25 min where; the oven was held at 60 °C for 2 min and then ramped to 300 °C with final hold of 7 min. The samples were injected with a split ratio of 30:1, and the injector port temperature was set at 250 °C with a constant linear velocity of 39 cm/s. Subsequently, MS ion source and interface temperature was set at, 200 and 280 °C, respectively. For SA extraction from human feces, 300 µl of methanol and 10 µl internal standards was added to accurately weighed 30 mg of human feces in triplicates. Samples were then sonicated for 30 min, followed by incubation at 37 °C with rpm of 1000 for another hour. These samples were then centrifuged at 25 °C for 5 min at 16,000 rcf, and 180 µl of supernatant was collected in respective GC vials. The SA was activated using DMT-MM and derivatized using *n*-octylamine and quantified using in-matrix linearity with internal standard calculation method with r^2 values ranging 98.9–99.9 for each SCFA. All the chemicals used for this analysis, including standards, were purchased from Sigma-Aldrich (India) of GCMS grade. The calculated concentrations were further adjusted to the respective sample dilution factor, further analysed and represented.

Collection of stool samples of UC patients. Stool samples from endoscopically active UC patients (endoscopic index of severity-UCEIS > 1) were collected and stored at −80 °C for metabolomics and metagenomics.

Isolation of lamina propria lymphocytes. Gut tissues were harvested and treated with 5 mM EDTA at 37 °C for 20 min to remove epithelial cells and dissociated in digestion buffer (IMDM, 1 mg/mL collagenase type VIII, 100 µg/mL DNase I, 5% FBS) with constant stirring at 37 °C for 30 min. Mononuclear cells were collected at the interface of a 40/80% Percoll gradient (GE Healthcare). Later Cells were analyzed by flow cytometry.

Data availability

All raw and processed data were presented in the supplementary tables. Any additional information that is required to reanalyze the data reported in this paper is available from the lead contact upon request.

Received: 23 September 2024; Accepted: 25 February 2025;
Published online: 13 March 2025

References

1. Fakhoury, M. et al. Inflammatory bowel disease: clinical aspects and treatments. *J. Inflamm. Res.* **7**, 113–120 (2014).
2. Chen, S. J. et al. Ulcerative colitis as a polymicrobial infection characterized by sustained broken mucus barrier. *World J. Gastroenterol.* **20**, 9468–9475 (2014).
3. Chandwaskar, R. et al. Dysregulation of T cell response in the pathogenesis of inflammatory bowel disease. *Scand. J. Immunol.* **100**, e13412 (2024).
4. Loscalzo, J. et al. in *Harrison's Principles of Internal Medicine* 21 edn 2022 (McGraw-Hill Education, 2022).
5. Wang, J. et al. Gut-microbiota-derived metabolites maintain gut and systemic immune homeostasis. *Cells* **12**, 293 (2023).
6. Deleu, S. et al. Short chain fatty acids and its producing organisms: an overlooked therapy for IBD? *EBioMedicine* **66**, 103293 (2021).
7. Barman, M. et al. Short-chain fatty acids (SCFA) in infants' plasma and corresponding mother's milk and plasma in relation to subsequent sensitisation and atopic disease. *EBioMedicine* **101**, 104999 (2024).
8. Miyamoto, J. et al. Nutritional signaling via free fatty acid receptors. *Int. J. Mol. Sci.* **17**, 450 (2016).
9. Le Poul, E. et al. Functional characterization of human receptors for short chain fatty acids and their role in polymorphonuclear cell activation. *J. Biol. Chem.* **278**, 25481–25489 (2003).
10. Singh, N. et al. Activation of Gpr109a, receptor for niacin and the commensal metabolite butyrate, suppresses colonic inflammation and carcinogenesis. *Immunity* **40**, 128–139 (2014).
11. Gasaly, N., Hermoso, M. A. & Gotteland, M. Butyrate and the fine-tuning of colonic homeostasis: implication for inflammatory bowel diseases. *Int. J. Mol. Sci*. **22**, 3061 (2021).
12. Fernández-Veledo, S. & Vendrell, J. Gut microbiota-derived succinate: friend or foe in human metabolic diseases? *Rev. Endocr. Metab. Disord.* **20**, 439–447 (2019).
13. Mirzaei, R. et al. Role of microbiota-derived short-chain fatty acids in nervous system disorders. *Biomed. Pharmacother.* **139**, 111661 (2021).
14. Fremder, M. et al. A transepithelial pathway delivers succinate to macrophages, thus perpetuating their pro-inflammatory metabolic state. *Cell Rep.* **36**, 109521 (2021).
15. Ren, W. et al. Slc6a13 deficiency promotes Th17 responses during intestinal bacterial infection.*Mucosol Immunol.* **12**, 1 (2018).
16. Khamaysi, A. et al. A dynamic anchor domain in slc13 transporters controls metabolite transport. *J. Biol. Chem.* **295**, 8155–8163 (2020).
17. Roy, S. et al. EGFR-HIF1α signaling positively regulates the differentiation of IL-9 producing T helper cells. *Nat. Commun*. **12** 2021.
18. Selak, M. A. et al. Succinate links TCA cycle dysfunction to oncogenesis by inhibiting HIF-α prolyl hydroxylase. *Cancer Cell* **7**, 77–85 (2005).
19. Ariza, A. C., Deen, P. & Robben, J. The succinate receptor as a novel therapeutic target for oxidative and metabolic stress-related conditions. *Front. Endocrinol*. **3**, 22 (2012).
20. Trauelsen, M. et al. Extracellular succinate hyperpolarizes M2 macrophages through SUCNR1/GPR91-mediated Gq signaling. *Cell Rep.* **35**, 109246 (2021).
21. Boursier, J. et al. The severity of nonalcoholic fatty liver disease is associated with gut dysbiosis and shift in the metabolic function of the gut microbiota. *Hepatology* **63**, 764–775 (2016).
22. Mills, E. L. et al. UCP1 governs liver extracellular succinate and inflammatory pathogenesis. *Nat. Metab.* **3**, 604–617 (2021).
23. Monfort-Ferré, D. et al. The gut microbiota metabolite succinate promotes adipose tissue browning in Crohn's disease. *J. Crohns Colitis* **16**, 1571–1583 (2022).
24. van Diepen, J. A. et al. SUCNR1-mediated chemotaxis of macrophages aggravates obesity-induced inflammation and diabetes. *Diabetologia* **60**, 1304–1313 (2017).

25. Osuna-Prieto, F. J. et al. Elevated plasma succinate levels are linked to higher cardiovascular disease risk factors in young adults. *Cardiovasc. Diabetol.* **20**, 151 (2021).
26. Serena, C. et al. Elevated circulating levels of succinate in human obesity are linked to specific gut microbiota. *ISME J.* **12**, 1642–1657 (2018).
27. Macias Ceja, D. et al. Succinate receptor mediates intestinal inflammation and fibrosis. *Mucosal Immunol.* **12**, 1 (2018).
28. Jiang, M. et al. Succinate and inosine coordinate innate immune response to bacterial infection. *PLoS Pathog.* **18**, e1010796 (2022).
29. Xu, J. et al. Succinate/IL-1β signaling axis promotes the inflammatory progression of endothelial and exacerbates atherosclerosis. *Front. Immunol.* **13**, 817572 (2022).
30. Tannahill, G. M. et al. Succinate is an inflammatory signal that induces IL-1β through HIF-1α. *Nature* **496**, 238–242 (2013).
31. Banerjee, A. et al. Succinate produced by intestinal microbes promotes specification of tuft cells to suppress ileal inflammation. *Gastroenterology* **159**, 2101–2115.e5 (2020).
32. Guo, Y. et al. Targeting the succinate receptor effectively inhibits periodontitis. *Cell Rep.* **40**, 111389 (2022).
33. Malik, S. & Awasthi, A. Transcriptional control of Th9 cells: role of Foxo1 in interleukin-9 induction. *Front. Immunol*. **9**, 995 (2018).
34. Sadhu, S. et al. IL-9 aggravates SARS-CoV-2 infection and exacerbates associated airway inflammation.*Nat. Commun.* **14**, 4060 (2023).
35. Hufford, M. & Kaplan, M. A gut reaction to IL-9. *Nat. Immunol.* **15**, 599–600 (2014).
36. Gerlach, K. et al. TH9 cells that express the transcription factor PU.1 drive T cell–mediated colitis via IL-9 receptor signaling in intestinal epithelial cells. *Nat. Immunol.* **15**, 676–686 (2014).
37. Yuan, C. et al. Interleukin-9 production by type 2 innate lymphoid cells induces Paneth cell metaplasia and small intestinal remodeling. *Nat. Commun.* **14**, 7963 (2023).
38. Zhang, J. et al. Association between succinate receptor SUCNR1 expression and immune infiltrates in ovarian cancer. *Front. Mol. Biosci*. **7**, 150 (2020).
39. Saraiva, A. L. et al. Succinate receptor deficiency attenuates arthritis by reducing dendritic cell traffic and expansion of Th17 cells in the lymph nodes.*FASEB J.* **32**, 6550–6558 (2018).
40. Dalal, R., Sadhu, S. & Awasthi, A. Role of Th17 cell in tissue inflammation and organ-specific autoimmunity. *Transl. Autoimmun.* **1**, 93–121 (2022).
41. Heller, F. et al. Oxazolone colitis, a Th2 colitis model resembling ulcerative colitis, is mediated by IL-13-producing NK-T cells. *Immunity* **17**, 629–638 (2002).
42. De Vadder, F. et al. Microbiota-produced succinate improves glucose homeostasis via intestinal gluconeogenesis. *Cell Metab.* **24**, 151–157 (2016).
43. Chen, Z. et al. Foxo1 controls gut homeostasis and commensalism by regulating mucus secretion. *J. Exp. Med*. **218**, e20210324 (2021).
44. Ferreyra, J. A. et al. Gut microbiota-produced succinate promotes C. difficile infection after antibiotic treatment or motility disturbance. *Cell Host Microbe* **16**, 770–777 (2014).
45. Boirivant, M. et al. Oxazolone colitis: a murine model of T helper cell type 2 colitis treatable with antibodies to interleukin 4. *J. Exp. Med.* **188**, 1929–1939 (1998).
46. Goto, H. et al. Effects of fructo-oligosaccharide on DSS-induced colitis differ in mice fed nonpurified and purified diets.*J. Nutr.* **140**, 2121–2127 (2010).
47. Wei, Y. H. et al. Succinate metabolism and its regulation of host-microbe interactions. *Gut Microbes* **15**, 2190300 (2023).
48. Zhou, X. et al. Intestinal accumulation of microbiota-produced succinate caused by loss of microRNAs leads to diarrhea in weanling piglets. *Gut Microbes* **14**, 2091369 (2022).
49. Matlac, D. M. et al. Succinate mediates tumorigenic effects via succinate receptor 1: potential for new targeted treatment strategies in succinate dehydrogenase deficient paragangliomas. *Front. Endocrinol.* **12**, 589451 (2021).
50. Wu, J. Y. et al. Cancer-derived succinate promotes macrophage polarization and cancer metastasis via succinate receptor. *Mol. Cell* **77**, 213–227.e5 (2020).
51. Kuo, C. C., Wu, J. Y. & Wu, K. K. Cancer-derived extracellular succinate: a driver of cancer metastasis. *J. Biomed. Sci.* **29**, 93 (2022).
52. Littlewood-Evans, A. et al. GPR91 senses extracellular succinate released from inflammatory macrophages and exacerbates rheumatoid arthritis. *J. Exp. Med.* **213**, 1655–1662 (2016).
53. Rizvi, Z. A. et al. High-salt diet mediates interplay between NK cells and gut microbiota to induce potent tumor immunity. *Sci. Adv.* **7**, eabg5016 (2021).
54. Hibberd, M. C. et al. The effects of micronutrient deficiencies on bacterial species from the human gut microbiota. *Sci. Transl. Med.* **9**, eaal4069 (2017).
55. Bloom, S. et al. Commensal bacteroides species induce colitis in host-genotype-specific fashion in a mouse model of inflammatory bowel disease. *Cell Host microbe* **9**, 390–403 (2011).
56. Tian, Y. et al. Vitamin A deficiency in mice alters host and gut microbial metabolism leading to altered energy homeostasis. J. *Nutr. Biochem*. **54**, 28–34 (2017).
57. Bonakdar, M. et al. Gut commensals expand vitamin A metabolic capacity of the mammalian host. *Cell Host Microbe* **30**, 1084–1092.e5 (2022).
58. Huang, H. et al. Cellular succinate metabolism and signaling in inflammation: implications for therapeutic intervention. *Front. Immunol.* **15**, 1404441 (2024).
59. Anthamatten, L. et al. Stratification of human gut microbiomes by succinotype is associated with inflammatory bowel disease status. *Microbiome* **12**, 186 (2024).
60. Pinget, G. V. et al. Dysbiosis in imiquimod-induced psoriasis alters gut immunity and exacerbates colitis development. *Cell Rep.* **40**, 111191 (2022).
61. Golub, L. M. & Lee, H. M. Periodontal therapeutics: current host-modulation agents and future directions. *Periodontol 2000* **82**, 186–204 (2020).
62. Bhuniya, D. et al. Discovery of a potent and selective small molecule hGPR91 antagonist. *Bioorg. Med. Chem. Lett.* **21**, 3596–3602 (2011).

Acknowledgements

We acknowledge the histological studies performed by Amit and his team at Biobank, ILBS, and by the SAF facility at THSTI by Dr. Bhisma Narayan Panda and team members Prabhanjan Dwivedi and Preeti. We are grateful for the invaluable help of Hardik Grover, Bhawna Verma, Manas Ranjan Tripathi, and Jitender Chandila during the study. We would like to express our gratitude to Dr. Bhabatosh Das and his student Bharti Singh for their invaluable assistance and generosity in allowing us to utilize their facility to cultivate the anaerobic bacteria. Their inputs and support have been instrumental in our research, and we are truly grateful for their cooperation. We express gratitude to CoTeRi, NIBMG for performing 16S rRNA metagenome analysis for our samples. We also acknowledge SAF-THSTI and "Immunology Core" of THSTI for providing the resources and support in conducting experiments and data analysis. Funding: We acknowledge the grant support provided by the National Bioscience award by DBT and the intramural grant by AIIMS-THSTI for this work. R.D. acknowledges the fellowship supported by DBT.

Author contributions

Conceptualization A.A.; Data curation: A.A.; Funding acquisition: A.A., Investigation: R.D., Methodology: R.D., S.S., D.K.R., K.C., Y.K.; Project administration: A.A., D.B.S., V.A.; Visualization: R.D., S.G., J.D., R.Y., V.S., V.K.D., R.K.; Writing: original draft: R.D., A.A.; Writing: review & editing: A.A.

Competing interests

The authors declare the filing of a provisional patent application in India (Indian Patent Application No.: 202311037041). The applicant is the Translational Health Science and Technology Institute (THSTI), India, with R.D. and A.A. listed as the inventors.

Additional information

Supplementary information The online version contains supplementary material available at https://doi.org/10.1038/s41522-025-00672-3.

Correspondence and requests for materials should be addressed to Amit Awasthi.